

國立交通大學

電信工程研究所

碩士論文



基於幾何方法欠定多輸入多輸出系統之  
高效率解碼演算法

Geometry Based Efficient Decoding Algorithm for  
Underdetermined MIMO Systems

研究生：吳智湧

Student: Chih-Yung Wu

指導教授：李大嵩 博士

Advisor: Dr. Ta-Sung Lee

中華民國九十九年六月

基於幾何方法欠定多輸入多輸出系統之  
高效率解碼演算法

Geometry Based Efficient Decoding Algorithm for  
Underdetermined MIMO Systems

研究生：吳智湧

Student: Chih-Yung Wu

指導教授：李大嵩 博士

Advisor: Dr. Ta-Sung Lee



A Thesis

Submitted to Institute of Communication Engineering  
College of Electrical and Computer Engineering  
National Chiao Tung University  
in Partial Fulfillment of the Requirements  
for the Degree of  
Master  
in

Communication Engineering

June 2010

Hsinchu, Taiwan, Republic of China

中華民國九十九年六月

# 基於幾何方法欠定多輸入多輸出系統之 高效率解碼演算法

學生：吳智湧

指導教授：李大嵩 博士

國立交通大學電信工程研究所

## 摘要

在多輸入多輸出系統中，高效率且低功率消耗之接收機的設計為關鍵議題之一。在多輸入多輸出系統中，球形解碼器是能有效提供最大似然的接收器。然而，典型球形解碼器無法運用在傳送天線個數大於接收天線個數的欠定系統中。針對此類系統，通用球形解碼被提出，但它的解碼複雜度隨著天線個數差的增加而呈現指數增加。在本論文中，針對此類欠定系統，吾人提出具有低解碼複雜度的解碼器。該解碼器包含了兩個步驟：1.藉由所提出的高效率的平面候選點搜尋器將所有所需的候選點一一找出。2.針對這些候選點集合進行平面交集的動作並配合動態半徑調整機制來快速地找出該問題的解。吾人亦提出一可與所提出解碼器結合之通道矩陣行向量的排序策略，進而提供低運算需求及近似最大似然搜尋的解碼性能。模擬結果顯示吾人提出方法的有效性。

# Geometry Based Efficient Decoding Algorithm for Underdetermined MIMO Systems

Student: Chih-Yung Wu

Advisor: Dr. Ta-Sung Lee

Institute of Communication Engineering

National Chiao Tung University

## Abstract

The design of high-performance and low-power consumption receiver is one of the key issues of MIMO systems. The sphere decoding algorithm (SDA) is an effective detector for MIMO systems. However, typical SDA fail to work in underdetermined MIMO systems where the number of transmit antennas is larger than the number of receive antennas. The generalized sphere decoder (GSD) had been proposed for underdetermined MIMO systems. However, its decoding complexity is exponentially increasing with the antenna number difference. In this thesis, we propose a decoder for underdetermined MIMO systems with low decoding complexity. The proposed decoder consists of two stages: 1. Obtaining all valid candidate points efficiently by slab decoder. 2. Finding the optimal solution by conducting the intersectional operations with dynamic radius adaptation to the candidate set obtained from Stage 1. We also propose a reordering strategy that can be incorporated into the proposed decoding algorithm to provide a lower computational complexity and near-ML decoding performance for underdetermined MIMO systems. Simulations confirm the effectiveness of the proposed methods.

# Acknowledgement

I would like to express my deepest gratitude to my advisors, Dr. Ta-Sung Lee, for his enthusiastic guidance and great patience. I learned a lot from his positive attitude in many areas, especially in the training of oral presentation. I thank Chester senior whose knowledge and experience have benefited me tremendously in my research. Thanks are also offered to all members in the Communication System Design and Signal Processing (CSDSP) Lab. Last but not least, I would like to show my sincere thanks to my family for their invaluable love and support.

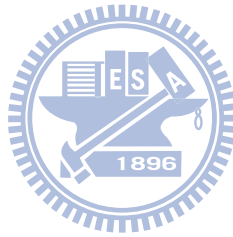
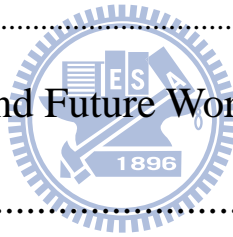


# Table of Contents

Chinese Abstract .....	I
English Abstract .....	II
Table of Contents .....	IV
List of Figures .....	VI
Acronym Glossary .....	VII
Notations.....	VIII
Chapter 1 Introduction.....	1
Chapter 2 Underdetermined MIMO System Model.....	4
2.1 System Model .....	5
2.2 Channel Capacity .....	6
2.3 MIMO Diversity .....	10
2.3.1 Receive Diversity.....	10
2.3.2 Transmit Diversity .....	11
2.4 Spatial Multiplexing.....	11
2.5 MIMO Detection.....	13
2.6 Underdetermined MIMO Detection.....	15
2.6.1 Generalized Sphere Decoder (GSD).....	15
2.6.2 Slab Sphere Decoding (SSD) Algorithm .....	17
2.7 Summary .....	23

Chapter 3	Proposed Geometry Based Decoding Algorithm with Intersection of Candidate Sets .....	24
3.1	Efficient Search Method for Points in Slab .....	25
3.2	Efficient Decoding Algorithm with Intersection of Candidate Sets.....	29
3.3	Computer Simulation .....	34
3.4	Summary .....	38
Chapter 4	Preprocessing of Proposed Decoding Algorithm.....	39
4.1	Preprocessing .....	40
4.2	Alternative Approach of Preprocessing .....	44
4.3	Computer Simulations .....	48
4.4	Summary .....	51
Chapter 5	Conclusions and Future Works .....	52
Bibliography	.....	54



# List of Figures

<b>Fig. 2-1</b> MIMO system block diagram .....	5
<b>Fig. 2-2</b> Spatial multiplexing system .....	12
<b>Fig. 2-3</b> Encoding procedure of D-BLAST ( $n=3$ ) .....	13
<b>Fig. 2-4</b> Encoding procedure of V-BLAST ( $n=3$ ) .....	13
<b>Fig. 3-1</b> An example of slab with 4-PAM and $k = 2$ .....	28
<b>Fig. 3-2</b> Block diagram of typical underdetermined decoding algorithms .....	29
<b>Fig. 3-3</b> Illustration of intersection of candidate sets .....	31
<b>Fig. 3-4</b> SER comparison of SSD and the proposed method using 16-QAM .....	36
<b>Fig. 3-5</b> Complexity comparison of SSD and the proposed method using 16-QAM.....	36
<b>Fig. 3-6</b> SER comparison of SSD and the proposed method using 64-QAM .....	37
<b>Fig. 3-7</b> Complexity comparison of SSD and the proposed method using 64-QAM.....	38
<b>Fig. 4-1</b> Geometrical diagram of slabs with different $y$ .....	41
<b>Fig. 4-2</b> Probability density function of $ y_m $ .....	47
<b>Fig. 4-3</b> The reduced percentage of Method I and Method II.....	48
<b>Fig. 4-4</b> SER comparison of proposed method with and without preprocessing .....	50
<b>Fig. 4-5</b> Complexity comparison of proposed method with and without preprocessing	50

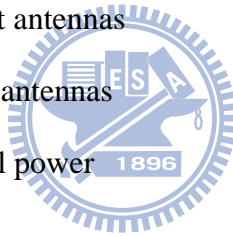


# Acronym Glossary

AWGN	additive white Gaussian noise
D-BLAST	diagonal Bell laboratories layered space-time
EGC	equal-gain combining
GSD	generalized sphere decoder
GS-QRD	Gram-Schmidt process-QR decomposition
Householder-QRD	Householder process-QR decomposition
MIMO	multiple-input multiple-output
ML	maximum-likelihood
MRC	maximum ratio combining
PDA	plane decoding algorithm
SDA	sphere decoding algorithm
SD	spatial diversity
SE	Schnorr and Euchner
SER	symbol-error-rate
SIC	successive interference cancellation
SISO	single-input-single-output
SLA	Slab Decoding Algorithm
SM	spatial multiplexing
SNR	signal-to-noise ratio
SSD	slab-sphere decoder
STC	space-time code
V-BLAST	vertical Bell laboratories layered space-time
ZF	zero-forcing

# Notations

$(\cdot)^T$	transpose operator
$\ \cdot\ $	2-norm operator
$E\{\cdot\}$	expectation operator
$\gamma(\cdot)$	lower incomplete Gamma function
$\Gamma(\bullet)$	Gamma function
$P(\bullet)$	regularized Gamma function
$C$	channel capacity
$\tilde{\mathbf{H}}$	complex channel matrix
$\mathbf{H}$	real channel matrix
$N_t$	number of transmit antennas
$N_r$	number of receive antennas
$P$	transmitted symbol power
$\tilde{\mathbf{n}}$	complex AWGN
$\mathbf{n}$	real AWGN
$\tilde{\mathbf{x}}$	complex transmitted signal vector
$\mathbf{x}$	real transmitted signal vector
$\tilde{\mathbf{y}}$	complex received signal vector
$\mathbf{y}$	real received signal vector



# Chapter 1

## Introduction

Recently, in order to satisfy the growing demands of the personal communications, the design of next generation wireless communication systems goes for supporting high data rate and high mobility. However, the link quality suffers from frequency selective and time selective fading caused by multipath propagation in wireless channels. Moreover, the quality and reliability of wireless communication are degraded by Doppler shift and carrier frequency/phase. Beside, due to the limited available bandwidth and transmitted power, the design challenge of wireless communication systems becomes more difficult. Therefore, many innovative techniques have been devised and extensively used in this field to improve the reliability and the spectral efficiency of wireless communication links e.g. the coded multicarrier modulation, smart antenna and multiple-input multiple-output (MIMO) technology [1-4] and adaptive modulation [5], [6].

Among these technologies, MIMO is the most outstanding one. MIMO technology involves the use of multiple antennas to improve link performance. There are two major features of MIMO technologies: spatial multiplexing for increasing data rate and spatial diversity for improve link quality. Spatial multiplexing offers a linear increasing of data rate by transmitting multiple independent data streams at the

same time. Spatial diversity provides diversity gain to mitigate fading effects by using the multiple (ideally independent) copies of the transmitted signal in space, time and frequency. They are usually trade-offs to each other and provide an effective and promising solution while achieving high-data rate and reliable transmission.

The major MIMO signal detection schemes include linear detection, successive interference cancellation (SIC) [7], [8] and the maximum-likelihood (ML) detection. The advantages of the first two detection schemes are low decoding complexity and easy implementation but their detection performances are non-optimal. ML detection provides optimal detection performance but its complexity increases exponentially with the size of constellation and the number of transmit antennas. Therefore, the design of high-performance and low decoding complexity is the one of key issues of MIMO designs. To reduce the complexity of the ML detector, the sphere decoding algorithm (SDA) [9], [10] has received considerable attention as an efficient detection scheme for MIMO systems. However, typical SDA fail to work in underdetermined MIMO systems where the number of transmit antennas is larger than the number of receive antennas.

To overcome the above drawbacks of typical SDA, the conventional generalized sphere decoder (GSD), double-layer sphere decoder (DLSD) and slab sphere decoder (SSD) are introduced in [11-15]. These decoders transform underdetermined systems into overdetermined systems that can be solved by the SDA. Since the GSD performs an exhaustive search on  $(N_t - N_r)$  dimensions for the ML solution, the decoding complexity is increasing with the size of constellation and the antenna number difference. The DLSD uses the outer sphere decoder to find the valid candidate points and then the inner sphere decoder uses those points to find the solution. The SSD uses the geometry concept to find the valid candidate points to reduce the searching complexity of DLSD. However, the SDA still needs to be performed too many times

in SSD.

In this thesis, our goal is to reduce the decoding complexity of the SSD without degrading the decoding performance. The proposed decoder consists of two stages: 1. Obtaining all valid candidate points efficiently by the slab decoder. 2. Finding the optimal solution by conducting the intersectional operations with dynamic radius adaptation to the candidate set obtained from Stage 1. We also propose a reordering strategy that can be incorporated into the proposed decoding algorithm to provide a lower computational complexity and near-ML decoding performance in underdetermined MIMO systems.

The organization of this thesis is given as follows. In Chapter 2, the signal model and typical detection schemes of overdetermined MIMO systems are introduced. In Chapter 3, the proposed decoder is presented. Two preprocessing scheme for the proposed decoder are suggested in Chapter 4. Simulation results are presented in both Chapter 3 and Chapter 4. Finally, Chapter 5 gives the conclusion and future works of this thesis.

# Chapter 2

## Underdetermined MIMO System Model

Many MIMO technologies are implemented in order to achieve the multiplexing gain and more diversity gain for wireless communication system. But in some scenarios (e.g. a strong LoS signal at receiver), an overdetermined MIMO system can be degraded into an underdetermined MIMO system. In underdetermined MIMO systems, the well-known SDA fail, therefore we need some special decoding schemes for these cases. In this chapter, those technologies of MIMO systems are introduced. We first introduce the MIMO system model in Section 2.1. Section 2.2 introduces the channel capacity. Second, the spatial diversity (SD) and the spatial multiplexing (SM) techniques are introduced in Section 2.3 and Section 2.4, respectively. Finally, the commonly used detection schemes for underdetermined MIMO systems including generalize sphere decoder (GSD), and Slab-sphere decoder (SSD) will be given in Section 2.5.

## 2.1 System Model

Consider a Gaussian MIMO system with  $N_t$  transmit antennas and  $N_r$  receive antennas as shown in **Fig. 2-1**. The relation between transmitted signal vector and received signal vector can be written as

$$\tilde{\mathbf{y}} = \tilde{\mathbf{H}}\tilde{\mathbf{x}} + \tilde{\mathbf{n}}, \quad (2.1)$$

where  $\tilde{\mathbf{y}} = [\tilde{y}_1, \tilde{y}_2, \dots, \tilde{y}_{N_r}] \in \mathbb{C}^{N_r \times 1}$  stands for the received signal vector,

$\tilde{\mathbf{x}} = [\tilde{x}_1, \tilde{x}_2, \dots, \tilde{x}_{N_t}] \in \mathbb{C}^{N_t \times 1}$  stands for the transmitted signal vector,  $\tilde{\mathbf{H}}$  stands for

the frequency-flat fading channel matrix:

$$\tilde{\mathbf{H}} = \begin{bmatrix} \tilde{h}_{1,1} & \tilde{h}_{1,2} & \dots & \tilde{h}_{1,N_t} \\ \tilde{h}_{2,1} & \tilde{h}_{2,2} & \dots & \tilde{h}_{2,N_t} \\ \vdots & \vdots & \ddots & \vdots \\ \tilde{h}_{N_r,1} & \tilde{h}_{N_r,2} & \dots & \tilde{h}_{N_r,N_t} \end{bmatrix} \in \mathbb{C}^{N_r \times N_t}, \quad (2.2)$$

where the elements of  $\tilde{\mathbf{H}}$  are complex i.i.d. Gaussian random variables with normal distribution  $CN(0,1)$  and  $\tilde{\mathbf{n}} = [\tilde{n}_1, \tilde{n}_2, \dots, \tilde{n}_{N_r}] \in \mathbb{C}^{N_r \times 1}$  stands for the complex

additive white Gaussian noise (AWGN) with normal distribution  $CN(0, \sigma^2 \mathbf{I})$ . It is

assumed  $n > m$  for an underdetermined MIMO systems.

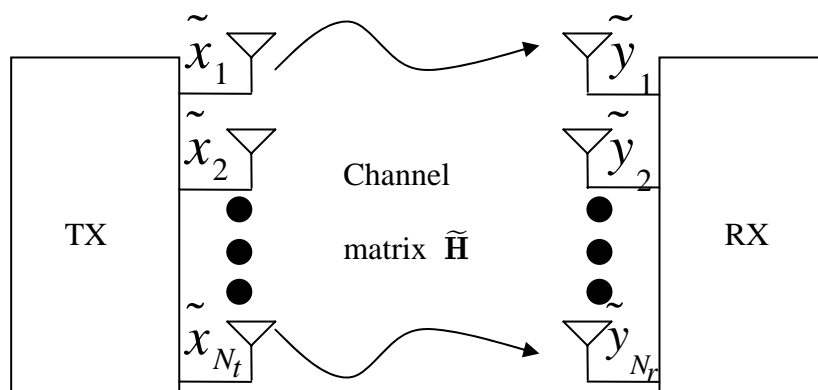


**Fig. 2-1** MIMO system block diagram

The complex equation in (2.1) can be rewritten into an equivalent real system by real value decomposition as

$$\mathbf{y} = \mathbf{H}\mathbf{x} + \mathbf{n}, \quad (2.3)$$

where

$$\begin{aligned} \mathbf{y} &= [\text{Re}\{\tilde{\mathbf{y}}\}^T \text{Im}\{\tilde{\mathbf{y}}\}^T] \in \mathbb{R}^M \\ \mathbf{x} &= [\text{Re}\{\tilde{\mathbf{x}}\}^T \text{Im}\{\tilde{\mathbf{x}}\}^T] \in \mathbb{R}^N \\ \mathbf{n} &= [\text{Re}\{\tilde{\mathbf{n}}\}^T \text{Im}\{\tilde{\mathbf{n}}\}^T] \in \mathbb{R}^M, \end{aligned} \quad (2.4)$$

and

$$\mathbf{H} = \begin{bmatrix} \text{Re}\{\tilde{\mathbf{H}}\}^T & -\text{Im}\{\tilde{\mathbf{H}}\}^T \\ \text{Im}\{\tilde{\mathbf{H}}\}^T & \text{Re}\{\tilde{\mathbf{H}}\}^T \end{bmatrix} \in \mathbb{R}^{M \times N}. \quad (2.5)$$

Note the  $\mathbf{H}$  is a size  $M \times N$  matrix where  $M = 2 \times N_r$  and  $N = 2 \times N_t$ .



## 2.2 Channel Capacity

Channel capacity is the upper bound of data rates in bits per channel that can be reliably transmitted over a communication channel. In other words, by channel coding theorem, if the data rate of transmission is below the channel capacity, the transmitted signals can be recovered with an arbitrarily small error probability. First, we introduce the single-input-single-output (SISO) channel capacity. Second, the MIMO channel capacity is introduced. The channel capacity is defined as [16]

$$C = \max_{p(x)} I(X;Y), \quad (2.6)$$

where

$$I(X;Y) = H(Y) - H(Y | X), \quad (2.7)$$

is the mutual information between  $X$  and  $Y$ , with  $H(Y)$  and  $H(Y|X)$  are the differential



entropy of  $Y$  and differential conditional entropy of  $Y$  with knowledge of  $X$  given, respectively. In (2.6), it states that the mutual information is maximized with respect to all possible transmitter statistical distributions  $p(x)$ .

## SISO Channel Capacity

For SISO systems, the ergodic capacity of a random channel can be defined as

$$C = E \left\{ \max_{p(x): P=1} I(X;Y) \right\}, \quad (2.8)$$

where  $P = E \left\{ |x(k)|^2 \right\}$  is transmitted symbol power over the channel,  $E \{ \cdot \}$  denotes the expectation of all channel realization, and the mutual information is equal to  $\log_2(1 + \gamma|h|^2)$ . The channel capacity defined in (2.8) means that the maximum of

mutual information between  $X$  and  $Y$  of all statistical distribution on the  $X$ . From (2.8), the SISO system ergodic capacity  $I(X;Y)$  can be replaced by  $\log_2(1 + \gamma|h|^2)$  [16]

$$C = E \left\{ \log_2(1 + \gamma|h|^2) \right\} \text{ bits/sec/Hz}, \quad (2.9)$$

where  $\gamma = P/\sigma^2$  is the average SNR at the receiver,  $P$  is the transmit power.

## MIMO Channel Capacity

For a MIMO system with  $N_t$  transmit antennas and  $N_r$  receive antennas, the ergodic capacity of a random MIMO channel can be defined as [1]

$$C = E \left\{ \max_{p(x): \text{tr}(\mathbf{R}_{xx})=N_t} I(X;Y) \right\}, \quad (2.10)$$

where  $\mathbf{R}_{xx} = E \left\{ \mathbf{x}\mathbf{x}^H \right\}$  is the covariance matrix of the transmitted signal vector  $\mathbf{x}$ .

Similar to SISO channel capacity, the MIMO mutual information can be described as

$$I(X;Y) = E \left\{ \log_2 \left[ \det \left( \mathbf{I}_{N_r} + \frac{P}{\sigma^2 N_t} \mathbf{H} \mathbf{R}_{xx} \mathbf{H}^H \right) \right] \right\}. \quad (2.11)$$

Substituting (2.11) into (2.10), we have

$$C = \max_{\text{tr}(\mathbf{R}_{xx})=N_t} E \left\{ \log_2 \left[ \det(\mathbf{I}_{N_r} + \frac{P}{\sigma^2 N_t} \mathbf{H} \mathbf{R}_{xx} \mathbf{H}^H) \right] \right\} \text{ bits/sec/Hz.} \quad (2.12)$$

When the channel knowledge is unknown to the transmitter, the optimal transmit signals are chosen to be independent and equal power. With independent and uniform power distribution, the covariance matrix of the transmit signal vector is then given by  $\mathbf{R}_{xx} = \mathbf{I}_{N_t}$ . As a result, the ergodic capacity of a MIMO system can be written as [1]

$$C = E \left\{ \log_2 \left[ \det(\mathbf{I}_{N_r} + \frac{P}{\sigma^2 N_t} \mathbf{H} \mathbf{H}^H) \right] \right\} \text{ bits/sec/Hz.} \quad (2.13)$$

By using the eigenvalue decomposition, the matrix product of  $\mathbf{H} \mathbf{H}^H$  can be decomposed as  $\mathbf{H} \mathbf{H}^H = \mathbf{E} \mathbf{\Lambda} \mathbf{E}^H$  where  $\mathbf{E}$  is an  $N_r \times N_r$  matrix which consists of the eigenvectors satisfying  $\mathbf{E} \mathbf{E}^H = \mathbf{E}^H \mathbf{E} = \mathbf{I}_{N_r}$  and  $\mathbf{\Lambda} = \text{diag}\{\lambda_1, \lambda_2, \dots, \lambda_{N_r}\}$  is a diagonal matrix with the eigenvalues  $\lambda_i \geq 0$  on the main diagonal. Assuming that the eigenvalues  $\lambda_i$  are ordered so that  $\lambda_i \geq \lambda_{i+1}$ , we have

$$\lambda_i = \begin{cases} \sigma_i^2, & \text{if } 1 \leq i \leq r \\ 0, & \text{if } r + 1 \leq i \leq N_r \end{cases}, \quad (2.14)$$

where  $\sigma_i^2$  is the  $i$ th squared singular value of the channel matrix  $\mathbf{H}$  and  $r = \text{rank}(\mathbf{H}) \leq \min\{N_t, N_r\}$  is the rank of the channel matrix. Then the capacity of a MIMO channel can be rewritten as

$$\begin{aligned} C &= E \left\{ \log_2 \left[ \det(\mathbf{I}_{N_r} + \frac{P}{\sigma^2 N_t} \mathbf{E} \mathbf{\Lambda} \mathbf{E}^H) \right] \right\} \\ &= E \left\{ \log_2 \left[ \det(\mathbf{I}_{N_r} + \frac{P}{\sigma^2 N_t} \mathbf{\Lambda}) \right] \right\} \\ &= \sum_{i=1}^r E \left\{ \log_2 \left( 1 + \frac{P}{\sigma^2 N_t} \lambda_i \right) \right\} \text{ bits/sec/Hz.} \end{aligned} \quad (2.15)$$

Note that the second equation holds due to the fact  $\det(\mathbf{I}_{N_r} + \mathbf{A}\mathbf{B}) = \det(\mathbf{I}_{N_t} + \mathbf{B}\mathbf{A})$  for matrices  $\mathbf{A} \in \mathbb{C}^{N_r \times N_t}$ ,  $\mathbf{B} \in \mathbb{C}^{N_t \times N_r}$  and  $\mathbf{E}^H \mathbf{E} = \mathbf{I}_{N_r}$ . Eq. (2.15) shows that the capacity of a MIMO channel is made up by the sum capacities of  $r$  independent SISO sub-channels with power gain  $\lambda_i$  for  $i = 1, 2, \dots, r$  and transmit power  $P/N_t$  individually.

When the channel knowledge is known to the transmitter, the capacity of a MIMO channel is the sum of the capacities associated with the independent SISO channels and is given by

$$C = \sum_{i=1}^r E \left\{ \log_2 \left( 1 + \gamma_i \frac{P}{\sigma^2 N_t} \lambda_i \right) \right\} \text{ bits/sec/Hz}, \quad (2.16)$$

where  $\gamma_i = E \left\{ |x_i|^2 \right\}$  for  $i = 1, 2, \dots, r$  is the transmit power in the  $i$ th sub-channel and  $\{\gamma_i\}$  satisfy the power constraint  $\sum_{i=1}^r \gamma_i = N_t$ . Since the transmitter can access the spatial sub-channels, we can allocate those powers across the sub-channels to maximize the mutual information as

$$C = \max_{\sum_{i=1}^r \gamma_i = N_t} \sum_{i=1}^r E \left\{ \log_2 \left( 1 + \gamma_i \frac{P}{\sigma^2 N_t} \lambda_i \right) \right\} \text{ bits/sec/Hz}, \quad (2.17)$$

the optimal power allocation of the  $i$ th sub-channel is a water-filling solution given by [1], [16]

$$\gamma_i^{\text{opt}} = \left( \mu - \frac{m\sigma^2}{P\lambda_i} \right)_+ \text{ for } i = 1, 2, \dots, r, \quad (2.18)$$

where  $\mu$  is chosen to satisfy the constraint  $\sum_{i=1}^r \gamma_i^{\text{opt}} = N_t$  and  $(\cdot)_+$  denotes the operation that takes those terms which are positive.

## 2.3 MIMO Diversity

Diversity techniques are widely used in MIMO systems to improve the reliability of transmission without increasing the transmit power or bandwidth. There are many diversity techniques such as space, frequency and time diversity. In this section the space diversity is introduced, it is so called antenna diversity.

### 2.3.1 Receive Diversity

Receive diversity involves the receiver with multiple antennas. At the receiver, multiple copies of the transmitted signal are received, which can be efficiently combined with an appropriate signal processing algorithm. There are four main types of combining techniques, include selection combining, switch combining, equal-gain combining (EGC) and the maximum ratio combining (MRC).

1. **Selection combining** – The received signal with the best quality is chosen and the choosing criterion is based on SNR.
2. **Switch combining** – Switch the received signal path to an alternative antenna when the current received signal level falls below a given threshold.
3. **EGC** – It is a simple method since it does not require estimation of the channel. The receiver simply combines the received signals from different receive antennas with weights set to be equal.
4. **MRC** – It forms the output signal by a linear combination of all the received signals and is the optimal combination technique which achieves the maximum value of the output SNR.

## 2.3.2 Transmit Diversity

Transmit diversity techniques provide more diversity benefits at the receiver with multiple transmit antennas, has received much attention, especially in wireless cellular systems. There are two broad categories of transmit diversity: the open loop schemes and the closed loop schemes. In the open loop schemes, the transmitter transmits signals without feedback information from receiver, e.g. Space-time code (STC). In the closed loop schemes, the transmitter transmits signals with feedback channel information from receiver, e.g. transmit beamforming.

## 2.4 Spatial Multiplexing

Spatial multiplexing is a transmission technique of MIMO wireless communication systems which increases the channel capacity without additional power or bandwidth, as shown in **Fig. 2-2**. In other words, spatial multiplexing means that transmit independent and separately data signals on each transmitted antenna in order to increase the channel capacity. If there are  $N_t$  antennas and  $N_r$  antennas of transmitter and receiver, respectively, the maximum spatial multiplexing order is

$$D = \min \{N_t, N_r\}, \quad (2.19)$$

if a linear receiver is used. This means that  $D$  data streams can be transmitted in parallel, the data rate can be increased by  $D$  times in the ideal case. The practical multiplexing gain is limited by correlation of channels, which means that some of the parallel streams may have very weak channel gains. Two typical spatial multiplexing schemes, D-BLAST [2] and V-BLAST [17] are introduced.

## Diagonal Bell Laboratories Layered Space-Time (D-BLAST)

The concept of layered space-time processing was proposed by Foschini at Bell Laboratories [2]. D-BLAST uses multiple antennas at both the transmitter and the receiver. The encoder uses a space time arrangement that corresponds to a diagonal layering. **Fig. 2-3** show the encoding procedure for D-BLAST.

## Vertical Bell Laboratories Layered Space-Time (V-BLAST)

The D-BLAST algorithm suffers from complicated implementation which is not suitable for practical situation. Therefore, a simplified version of the BLAST algorithm is known as V-BLAST [17]. In V-BLAST system, independently encoded data streams are transmitted from each transmit antenna simultaneously. The encoding procedure is shown in **Fig. 2-4**.

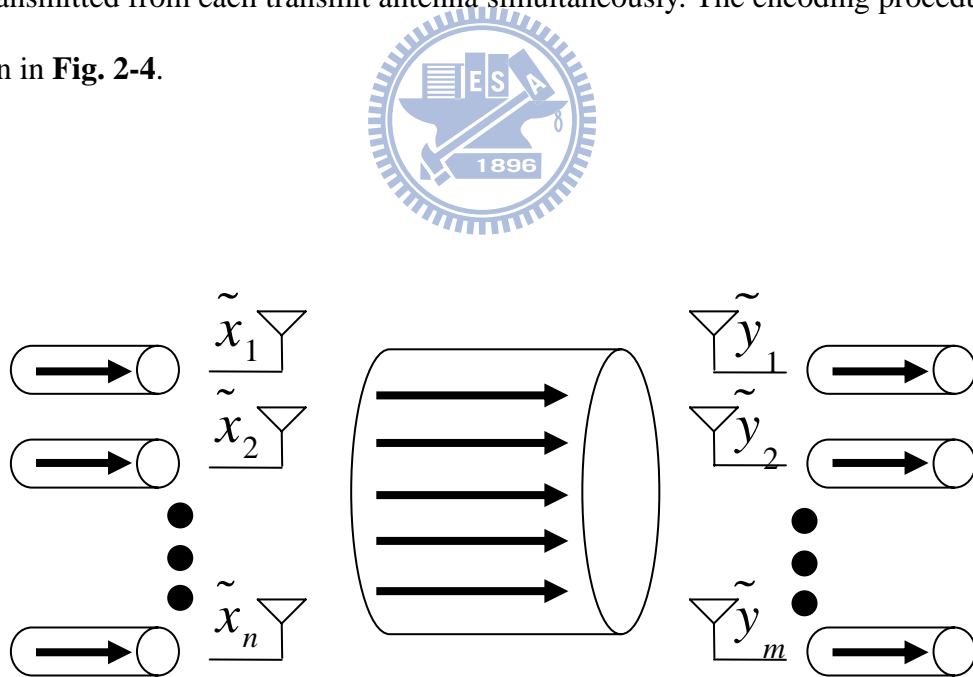


**Fig. 2-2** Spatial multiplexing system

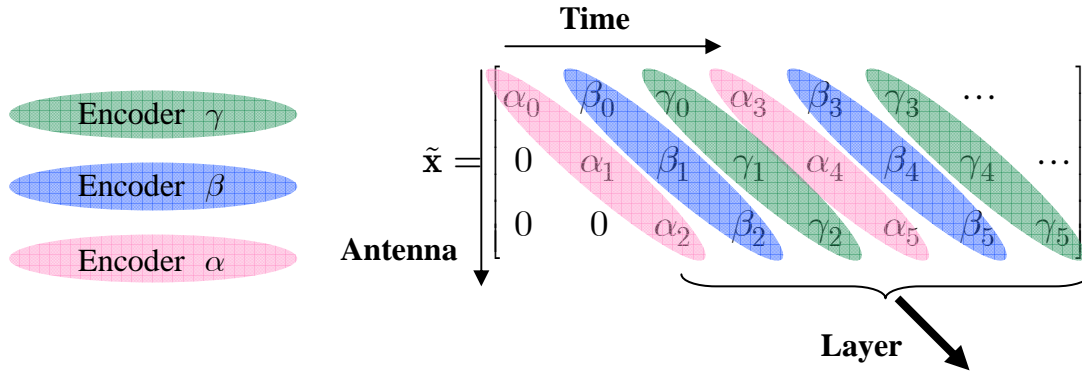


Fig. 2-3 Encoding procedure of D-BLAST ( $n=3$ )

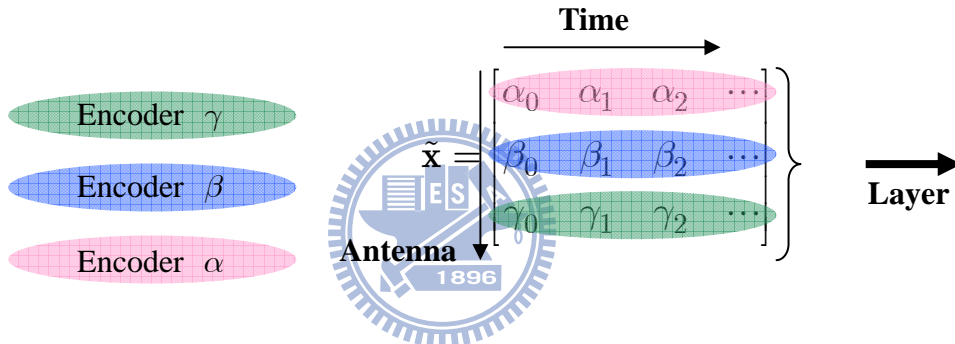


Fig. 2-4 Encoding procedure of V-BLAST ( $n=3$ )

## 2.5 MIMO Detection

In this section, we introduce the classification of MIMO detection schemes including Zero-Forcing (ZF), Zero-Forcing Successive Interference Cancellation (ZF-SIC) and Maximum-Likelihood (ML) detection. Assume that the received signal is given by (2.3)

$$\mathbf{y} = \mathbf{H}\mathbf{x} + \mathbf{n}. \quad (2.20)$$

## (1) Zero-Forcing (ZF)

The ZF scheme is a kind of linear detection that means the received signal  $\mathbf{y}$  is multiplied by a filter  $\mathbf{G}_{\text{ZF}}$

$$\mathbf{G}_{\text{ZF}} = (\mathbf{H}^H \mathbf{H})^{-1} \mathbf{H}^H = \mathbf{H}^\dagger, \quad (2.21)$$

where  $\mathbf{H}^\dagger$  is the Moore-Penrose pseudo-inverse of  $\mathbf{H}$ . The output vector after the filter is as follows

$$\tilde{\mathbf{y}} = \mathbf{H}^\dagger \mathbf{y}. \quad (2.22)$$

The ZF can remove the spatial interferences from the received signal; however, the main drawback of ZF scheme is the resulting noise enhancement.

## (2) Zero-Forcing Successive Interference Cancellation (ZF-SIC)

Denote  $\mathbf{H}$  as


$$\mathbf{H} = [\tilde{\mathbf{h}}_1, \dots, \tilde{\mathbf{h}}_{N_t}]. \quad (2.23)$$

The received signal is given by

$$\mathbf{y} = \mathbf{H}\mathbf{x} + \mathbf{n} = x_1 \mathbf{h}_1 + x_2 \mathbf{h}_2 + \dots + x_{N_t} \mathbf{h}_{N_t} + \mathbf{n}. \quad (2.24)$$

The main idea of SIC is to cancel the detected symbol from the received signal to improve primary ZF detection performance. The ZF filter is given in (2.21). The decision statistics of the  $i$ th symbol is obtained as

$$\hat{x}_i = \mathbf{H}_i^\dagger \mathbf{y}, \quad (2.25)$$

where  $\mathbf{H}_i^\dagger$  is the  $i$ th row of  $\mathbf{H}^\dagger$ . Taking hard decision to  $\hat{x}_i$ , the estimation symbol  $\hat{s}_i$  can be obtained. After  $\hat{s}_i$  is detected, it is subtracted from the received signal to remove its influence, then updating the received signal as

$$\mathbf{y}' = \mathbf{y} - \hat{s}_i \mathbf{h}_i, \quad (2.26)$$



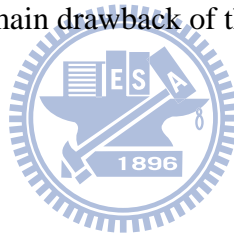
where  $\mathbf{h}_i$  is the  $i$ th column in the channel matrix  $\mathbf{H}$ . Iterating the above procedure, the ZF-SIC solution can be achieved.

### (3) Maximum-Likelihood (ML) Detection

The well known optimal detection scheme of the MIMO systems is the ML detection. The ML detection searches all possible combinations of transmitted symbols via the following criterion:

$$\hat{\mathbf{x}}_{\text{ML}} = \arg \min_{\mathbf{x} \in \mathbb{Z}^N} \|\mathbf{y} - \mathbf{H}\mathbf{x}\|^2, \quad (2.27)$$

where  $\mathbb{Z}^N$  denotes the set of all possible transmitted symbol vectors. The computational complexity of an exhaustive searching algorithm for the ML solution increases exponentially with  $N$ . Therefore, it is not easy to be implemented at the receiver in practice which is the main drawback of this method.



## 2.6 Underdetermined MIMO Detection

The classification of underdetermined MIMO detection schemes (e.g. GSD and SSD) are introduced in this section

### 2.6.1 Generalized Sphere Decoder (GSD)

In order to reduce the complexity of ML detection, the SDA was proposed to achieve ML performance with low complexity. Hence, it is adopted on the receiver design in recent years. But the SDA fails in the underdetermined MIMO systems and then the GSD [11] was proposed to solve this problem. The GSD transforms

underdetermined systems to overdetermined system that can be solved by SDA [19].

Consider a Gaussian MIMO system with  $N_t$  transmitted antennas and  $N_r$  received antennas, the received real signal can be formed as (2.3). The ML estimator  $\hat{\mathbf{x}}$  of  $\mathbf{x}$  is obtained by minimizing the Euclidean distance of  $\mathbf{y}$  from the legal lattice points as

$$\hat{\mathbf{x}} = \arg \min_{\mathbf{x} \in \mathbb{Z}^N} \|\mathbf{y} - \mathbf{H}\mathbf{x}\|^2 = \arg \min_{\mathbf{x} \in \mathbb{Z}^N} \|\mathbf{R}(\rho - \mathbf{x})\|^2. \quad (2.28)$$

where  $\mathbb{Z} = \{-3, -1, 1, 3\}$  for 16-QAM cases,  $\rho = \mathbf{H}^T (\mathbf{H}\mathbf{H}^T)^{-1} \mathbf{y}$ ,  $\mathbf{Q}$  is a  $M \times M$  unitary matrix, and  $\mathbf{R}$  is a  $M \times N$  upper triangular matrix corresponding to the QR-decomposition of  $\mathbf{H}$ , i.e.  $\mathbf{H} = \mathbf{Q}\mathbf{R}$ . The matrix  $\mathbf{R}$  can be represented by

$\mathbf{R} = [\mathbf{R}_1, \mathbf{R}_2]$ , where  $\mathbf{R}_1 \in \mathbb{R}^{M \times M}$  is a upper triangular matrix and  $\mathbf{R}_2 \in \mathbb{R}^{M \times N-M}$ . Similarly,  $\mathbf{x}$  can be represented by  $\mathbf{x} = [\mathbf{x}_G, \mathbf{x}_{\bar{G}}]^T$ , where  $G$  and  $\bar{G}$  are the indices corresponding to the first  $M$  and the last  $N - M$  elements of the

$\mathbf{x}$  vector. The minimum distance corresponding to the ML estimator in (2.28) can be rewritten by

$$\begin{aligned} & \arg \min_{\mathbf{x} \in \mathbb{Z}^N} \|\mathbf{R}(\rho - \mathbf{x})\|^2 \\ &= \min_{\mathbf{x}_{\bar{G}} \in \mathbb{Z}^{N-M}} \left( \min_{\mathbf{x}_G \in \mathbb{Z}^M} \left\| [\mathbf{R}_1, \mathbf{R}_2] \rho - \mathbf{R}_2 \mathbf{x}_{\bar{G}} - \mathbf{R}_1 \mathbf{x}_G \right\|^2 \right) \\ &= \min_{\mathbf{x}_{\bar{G}} \in \mathbb{Z}^{N-M}} \left( \min_{\mathbf{x}_G \in \mathbb{Z}^M} \left\| \tilde{\rho} - \mathbf{R}_1 \mathbf{x}_G \right\|^2 \right), \end{aligned} \quad (2.29)$$

where  $\tilde{\rho} = [\mathbf{R}_1, \mathbf{R}_2] \rho - \mathbf{R}_2 \mathbf{x}_{\bar{G}}$  for the last equation.

The GSD checks all the valid constellation points whose squared Euclidean distance calculated from (2.28) are smaller than a specified positive number  $C$ . It is done by an exhaustive search over  $\mathbf{x}_{\bar{G}}$  and then employing the SDA to compute the

last equation in (2.29). The SDA will find if the squared minimum distance is less than  $C$ . Otherwise, a failure of the SDA for the given  $\mathbf{x}_{\bar{G}}$  is declared and then the  $\mathbf{x}_{\bar{G}}$  will be discarded.

If the candidate constellation point  $(\mathbf{x}_G, \mathbf{x}_{\bar{G}})$  is found within the sphere, the value of  $C$  will be updated and the algorithm continues to search the remaining points for  $\mathbf{x}_{\bar{G}}$ . If no candidate constellation point  $(\mathbf{x}_G, \mathbf{x}_{\bar{G}})$  is found within the sphere, then the entire algorithm will repeat with a larger value of the radius  $C$ . The GSD based on the exhaustive search over  $\mathbf{x}_{\bar{G}}$  and the SDA for every point of. Because of the exhaustive search over  $\mathbf{x}_{\bar{G}}$ , the complexity exponentially increase of the order  $N - M$ .



## 2.6.2 Slab Sphere Decoding (SSD) Algorithm

To perform (2.28) efficiently, an algorithm is proposed in [18], [19] to solve a search problem that finds all the lattice points satisfying

$$\|\mathbf{y} - \mathbf{H}\mathbf{x}\|^2 \leq C^2 \quad (2.30)$$

for given a radius  $C (>0)$ . Apparently, the point that is the closest to center of the hypersphere  $\mathbf{y}$ , is the ML decision point. By decomposing the channel using QR-decomposition, Eq. (2.30) can be rewritten as

$$\|\mathbf{y}' - \mathbf{R}\mathbf{x}\|^2 \leq C^2, \quad (2.31)$$

where  $\mathbf{y}' = \mathbf{Q}^T \mathbf{y}$ .

If  $N > M$  we will have

$$-C \leq y'_M - [r_{M,M}x_M + \dots + r_{M,N}x_N] \leq C, \quad (2.32)$$

at the  $M$ th layer. Eq. (2.32) involves  $N-M+1$  dimensions for detection. Eq. (2.32) is similar to a detection problem of a real-valued MISO system. First, we want to find the constellation points falling inside this slab. There are two algorithms that can help us find those constellation points, i.e., Plane Decoding Algorithm (PDA) [12] and Slab Decoding Algorithm (SLA) [14], [15].

## Plane Decoding

For a MISO system with  $k$  transmitted antennas where the inputs are independent symbols, the received signal can be written as

$$y = h_1x_1 + \dots + h_kx_k + \eta, \quad (2.33)$$

where  $x_k \in \mathbb{Z}$ ,  $h_n$  is the channel response and  $\eta \sim CN(0, \sigma^2)$  stands for AWGN.

ML estimation of the transmitted vector  $\mathbf{x} = [x_1, \dots, x_k]$  can be written as

$$\mathbf{x}_{ML} = \arg \min_{(x_1, \dots, x_k) \in \mathbb{Z}^k} (y - h_1x_1 + \dots + h_kx_k)^2, \quad (2.34)$$

the estimator means to find the point  $\mathbf{x} \in \mathbb{Z}^k$  which is the closest to the hyperplane  $P$  given as

$$P : h_1x_1 + \dots + h_kx_k = y. \quad (2.35)$$

First, define  $X$ ,  $X_V$ ,  $X_{PD}$  as the sets of the points to be visited, the points that have been visited, and the points that are close to  $P$  in all dimensions, respectively.

Then, initialize them with  $X = X_V = \{\mathbf{x}^{(1)}\}$  where the (1) stands for the order of the vector in a set and  $j = 1$ .

The main idea of the PDA is to find those candidates ( $X_{PD}$ ) which are close to  $P$  in all dimensions. The procedures of the PDA are summarized as follows:

Step 1: If  $X$  is empty, go to Step 5. Otherwise, we calculate

$$\hat{a}_j = \left\{ x : \min_{x \in \mathbb{Z}} x \text{ s.t. } x > x_B \right\}$$

$$\tilde{a}_j = \left\{ x : \max_{x \in \mathbb{Z}} x \text{ s.t. } x < x_B \right\},$$

where

$$x_B = x_j^{[1]} - \frac{\Delta y(\mathbf{x}^{(1)})}{|h_j|}$$

$$\Delta y(\mathbf{x}^{(1)}) = |h_1|x_1^{[1]} + |h_2|x_2^{[1]} + \dots + |h_k|x_k^{[1]} - y$$

Step 2: If  $\{\hat{a}_k \neq \Phi\} \wedge \{\tilde{a}_k = \Phi\}$  is not true, go to Step 3. Otherwise, we have the point  $\hat{\mathbf{x}} = \mathbf{x}^{(1)}$  except that  $\hat{x}_j = \hat{a}_j$  where  $\hat{\mathbf{x}}$  is close to  $P$  in dimension- $j$ . Then, if  $\hat{x}_j = x_j^{(1)}$  and then the point  $\mathbf{x}^{(1)}$  is close to  $P$  in dimension-1,2,..., $j$  and do:

- If  $j < k$ , update  $j = j + 1$ . Go to Step 1.
- If  $j = k$ , the point  $\mathbf{x}^{(1)}$  is close to  $P$  in all dimensions and is stored in  $X_{PD}$ . Next, discard  $\mathbf{x}^{(1)}$  from the set  $X$  and reset  $j = 1$ . Go back to Step 1 to check a new point in  $X$ .

Else, if  $\hat{x}_j \neq a_j^{(1)}$ , then discard  $\mathbf{x}^{(1)}$  from the set  $X$  and reset  $j = 1$ .

Go back to Step 1.

Step 3: If  $\{\hat{a}_k = \Phi\} \wedge \{\tilde{a}_k \neq \Phi\}$  is not true, go to Step 4. Otherwise, we have the point  $\tilde{\mathbf{x}} = \mathbf{x}^{(1)}$  except that  $\tilde{x}_j = \tilde{a}_j$  where  $\tilde{\mathbf{x}}$  is close to  $P$  in dimension- $j$ . Then, if  $\tilde{x}_j = x_j^{(1)}$  and then the point  $\mathbf{x}^{(1)}$  is close to  $P$  in dimension-1,2,..., $j$  and do:

- If  $j < k$ , update  $j = j + 1$ . Go to Step 1.
- If  $j = k$ , the point  $\mathbf{x}^{(1)}$  is close to  $P$  in all dimensions and is stored in  $X_{PD}$ . Next, discard  $\mathbf{x}^{(1)}$  from the set  $X$  and reset  $j = 1$ . Go back to Step 1 to check a new point in  $X$ .

Else, if  $\tilde{x}_j \neq a_j^{(1)}$ , then discard  $\mathbf{x}^{(1)}$  from the set  $X$  and reset  $j = 1$ .

Go back to Step 1.

Step 4: If  $\{\hat{a}_k \neq \Phi\} \wedge \{\tilde{a}_k \neq \Phi\}$  is not true, go to Step 5. Otherwise, we have two points  $\hat{\mathbf{x}} = \mathbf{x}^{(1)}$  except that  $\hat{x}_j = \hat{a}_j$  and  $\tilde{\mathbf{x}} = \mathbf{x}^{(1)}$  except that  $\tilde{x}_j = \tilde{a}_j$  where  $\hat{\mathbf{x}}$  and  $\tilde{\mathbf{x}}$  are close to  $P$  in dimension- $j$ . Then, if  $\hat{x}_j = x_j^{(1)}$  and then the point  $\mathbf{x}^{(1)}$  is close to  $P$  in dimension-1,2,..., $j$  and do:

- If  $j < k$ , update  $j = j + 1$  and if  $\tilde{\mathbf{x}} \notin X_V$  then update  $X = \{X, \tilde{\mathbf{x}}\}$  and  $X_V = \{X_V, \tilde{\mathbf{x}}\}$ . Go to Step 1.
- If  $j = k$ , the point  $\mathbf{x}^{(1)}$  is close to  $P$  in all dimensions and is stored in  $X_{PD}$ . Next, discard  $\mathbf{x}^{(1)}$  from the set  $X$  and reset  $j = 1$ . Go back to Step 1 to check a new point in  $X$ .

If  $\tilde{x}_j = x_j^{(1)}$  and then do:

- If  $j < k$ , update  $j = j + 1$  and if  $\hat{\mathbf{x}} \notin X_V$  then update  $X = \{X, \hat{\mathbf{x}}\}$  and  $X_V = \{X_V, \hat{\mathbf{x}}\}$ . Go to Step 2.
- If  $j = k$ , the point  $\mathbf{x}^{(1)}$  is close to  $P$  in all dimensions and is stored in  $X_{PD}$ . Next, discard  $\mathbf{x}^{(1)}$  from the set  $X$  and reset  $j = 1$ . Go back to Step 1 to check a new point in  $X$ .

Else, if  $x_j^{(1)} \neq \hat{a}_j, \tilde{a}_j$ , then discard  $\mathbf{x}^{(1)}$  from the set  $X$  and reset  $j = 1$ .

Go back to Step 1.

Step 5: Each point  $\mathbf{x}$  in  $X_{PD}$ , update

$$x_k = -x_k \quad \forall k \text{ if } h_k < 0.$$

The PDA guarantees to achieve the ML solution only for the MISO systems. For MIMO systems, we will need to find those points that fall inside the slab

$$-C \leq y - [h_1 x_1 + \dots + h_k x_k] \leq C, \quad (2.36)$$

The following algorithm is designed to accomplish this.

## Slab Decoding

Obviously, although the  $X_{PD}$  does not contain all the lattice points that fall inside the slab in (2.36), the  $X_{PD}$  provides a useful starting point for slab detection.

The procedures of SDA are summarized as follows:

Step 1: Sorting the points of  $X_{PD}$  according to their Euclidean distances. Therefore,

$$X_{PD}^{\text{sort}} = \{\mathbf{x}_{PD}^{(1)}, \mathbf{x}_{PD}^{(2)}, \mathbf{x}_{PD}^{(3)}, \dots\}$$

where  $\Delta y^2(\mathbf{x}_{PD}^{(i)}) \leq \Delta y^2(\mathbf{x}_{PD}^{(j)})$  if  $i \leq j$ .

Step 2: For a given  $C$ , find the set

$$X_{PD; \leq C^2} = \{\mathbf{x} \in X_{PD}^{\text{sort}} : -C \leq \Delta y(\mathbf{x}) \leq C\}$$

Step 3: For each point  $\mathbf{x} \in X_{PD; \leq C^2}$ , move away along each direction for finding other points which  $\Delta y^2(\mathbf{x}) \leq C^2$ . It is done by the following loop.

a. Initialize  $n = 1$ , and  $j = 1$ . Pick the  $n$ th point  $\mathbf{u}^{(n)} \in X_{PD; \leq C^2}$ .

b. Compute

$$u_0 = \min \left( u_j^{(n)} + d, \max_{s \in \mathbb{Z}} s \right),$$

where  $d$  stands for the separation of every adjacent constellation.

If  $u_j^{(n)} \neq u_0$  and then do the following.

- Set  $u_j^{(n)} = u_0$ .
- If  $\Delta y^2(\mathbf{u}^{(n)}) \leq C^2$ , then  $X_{PD; \leq C^2} = \{X_{PD; \leq C^2}, \mathbf{u}^{(n)}\}$ .

c. Compute

$$u_0 = \max \left( u_j^{(n)} + d, \min_{s \in \mathbb{Z}} s \right).$$

If  $u_j^{(n)} \neq u_0$  and then do the following.

- Set  $u_j^{(n)} = u_0$ .
- If  $\Delta y^2(\mathbf{u}^{(n)}) \leq C^2$ , then  $X_{PD; \leq C^2} = \{X_{PD; \leq C^2}, \mathbf{u}^{(n)}\}$ .

d. If  $j < k$ , then update  $j = j + 1$  and go back to b.

e. If  $j = k$ , then update  $n = n + 1$  and  $j = 1$ . Then, go back to b.

f. If  $n = |X_{PD; \leq C^2}|$ , then all lattice points that fall inside the slab are found.

The two algorithms can find all the lattice points satisfying (2.36) for a given  $C$ .

Each point of the set can be substituted into the original problem in (2.31), to obtain

$$\|\mathbf{y}_G - \mathbf{R}_1 \mathbf{x}_G\|^2 \leq C^2 \quad (2.37)$$

where  $\mathbf{y}_G \in \mathbb{R}^{M-1}$ ,  $\mathbf{R}_1 \in \mathbb{R}^{M-1 \times M-1}$  corresponds to the first  $M-1$  columns

and rows of the  $\mathbf{R}$  and  $\mathbf{x}_G = [x_1, x_2, \dots, x_{M-1}] \in \mathbb{R}^{M-1}$ . Since  $\mathbf{R}_1$  is an upper

triangular matrix with full rank, we can solve the problem by SDA directly. After the

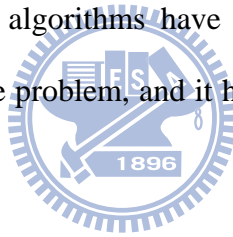
substitution of all points, the ML solution can be found.



## 2.7 Summary

In this Chapter, we review the MIMO communication systems. In a rich multi-path scattering environment, the MIMO system deliver significant performance enhancement in terms of link quality and data rate. Spatial diversity is a key MIMO technique which mitigates fading and is realized by providing the receiver with multiple copies of the transmitted signal in space or time. Spatial multiplexing offer a linear increase in data rate by transmitting independent data streams from the individual transmit antennas.

Two popular detectors of underdetermined MIMO systems are GSD and SSD. The complexity of GSD increases exponentially with the order of  $N - M$ . In order to reduce the complexity many algorithms have been proposed. The SSD uses a geometrical approach to solve the problem, and it has lower complexity than existing algorithms.



## Chapter 3

# Proposed Geometry Based Decoding Algorithm with Intersection of Candidate Sets

In Chapter2, we introduce the SSD which is a low complexity solution for underdetermined systems; however, the SSD has some disadvantages. First, because the two algorithms of SSD are independently and sequentially implemented, many constellation points are multiply checked. Second, in the PDA of SSD, in order to find the “ $X_{PD}$ ”, we perform many searches in the same dimension. As a result there are too many candidate points that fall inside the slab such that the SDA is executed too many times. For those reasons, its computational complexity is high.

In this chapter, we introduce the proposed a low complexity search method for finding those points falling inside the slab and a low complexity decoding algorithm without the use of SDA. The details of the proposed algorithm will be introduced in Sections 3.1-3.2. The simulation results will be provided in Section 3.3 to show that the proposed algorithm performs better than the SSD.

### 3.1 Efficient Search Method for Points in Slab

The search method is similar to the PDA and SLA. We use only one algorithm to find those points that fall inside the slab, so no constellation points and dimensions are multiply searched. First, performing QR-decomposition to the real channel matrix  $\mathbf{H}$ , we obtain

$$\mathbf{H} = \mathbf{QR}, \quad (3.1)$$

where  $\mathbf{Q} \in \mathbb{R}^{M \times N}$  and  $\mathbf{R}$  is an  $M \times N$  upper triangular matrix. Substituting (3.1) into (2.30), we have

$$\|\mathbf{y}' - \mathbf{R}\mathbf{x}\|^2 \leq C^2, \quad (3.2)$$

where  $\mathbf{y}' = \mathbf{Q}^T \mathbf{y}$ . If  $N > M$ , we will have

$$-C \leq y'_M - [r_{M,M}x_M + \dots + r_{M,N}x_N] \leq C, \quad (3.3)$$

at the  $M$ -th layer. Eq.(3.3) involves  $N-M+1$  dimensions for detection. The algorithm still aims to find those points that fall inside the slab.

First, define as

$$\text{Dist}_i = \left\| \begin{bmatrix} y'_i \\ y'_{i+1} \\ \vdots \\ y'_M \end{bmatrix} - \begin{bmatrix} r_{i,i} & r_{i,i+1} & \cdots & r_{i,M} & r_{i,M+1} & \cdots & r_{i,N} \\ 0 & r_{i+1,i+1} & \cdots & r_{i+1,2M} & r_{i+1,M+1} & \cdots & r_{i+1,N} \\ \vdots & \cdots & \ddots & \ddots & \ddots & \ddots & \vdots \\ 0 & \cdots & 0 & r_{M,M} & r_{M,M+1} & \cdots & r_{M,N} \end{bmatrix} \begin{bmatrix} x_i \\ x_{i+1} \\ \vdots \\ x_N \end{bmatrix} \right\|, \quad (3.4)$$

where  $1 \leq i \leq M$ .

Second, define as  $X_{\text{in}}$ ,  $X_{V_{\text{in}}}$ ,  $X_{V_{\text{out}}}$ ,  $D_{V_{\text{in}}}$ ,  $D_{V_{\text{out}}}$ ,  $X_{VD}$  the set of the points inside the slab, the sets of the points inside the slab to be visited, the sets of the points outside the slab to be visited, the visited dimensions of  $X_{V_{\text{in}}}$ , the visited dimensions

of  $X_{V_{\text{out}}}$  and the points that have been visited, respectively. Then, initialize them with  $X_{V_{\text{out}}} = X_{VD} = \{\mathbf{x}_{\text{out}}^{(1)}\}$  where the superscript (1) stands for the order of the vector in a set,  $j = 1$ , and  $D_{V_{\text{out}}} = [0, 0, \dots, 0]$  indicates that no dimension is visited in the beginning.

The main idea of the algorithm is to find those point ( $X_{\text{in}}$ ) which fall into the slab (3.3). We design an algorithm to find the set  $X_{\text{in}}$  efficiently and the procedures of the search algorithm are summarized as follows.

Step 1: If  $X_{V_{\text{in}}}$  and  $X_{V_{\text{out}}}$  are empty, go to Step 5.

Step 2: If  $X_{V_{\text{out}}}$  is empty, go to Step 4. Otherwise, we calculate

$$x_{j,\text{up}} = x_{j,\text{out}}^{(1)} - \frac{\Delta y(\mathbf{x}^{(1)})}{h_j} + C$$

$$x_{j,\text{low}} = x_{j,\text{out}}^{(1)} - \frac{\Delta y(\mathbf{x}^{(1)})}{h_j} - C,$$

where  $j$  is chosen from the unvisited dimension of  $D_{V_{\text{out}}}$  corresponding to each  $x$ .

Step 3: For each value  $x \in \{[x_{j,\text{low}}, x_{j,\text{up}}] \cap \mathbb{Z}^1\}$  and then we have the points

$\hat{\mathbf{x}} = \mathbf{x}^{(1)}$  where  $\hat{x}_j = x$ , and  $\hat{\mathbf{x}}$  is inside the slab.

● Update the  $j$ th element of  $D_{V_{\text{in}}}$  corresponding to each  $\hat{\mathbf{x}}$ . If

$$\hat{\mathbf{x}} \notin X_{V_{\text{in}}} \text{ then } X_{V_{\text{in}}} = \{X_{V_{\text{in}}}, \hat{\mathbf{x}}\}.$$

And the value  $a \in \{\{\hat{a}_j : \max(x) + d, \hat{a}_k : \min(x) - d\} \cap \mathbb{Z}^1\}$  where

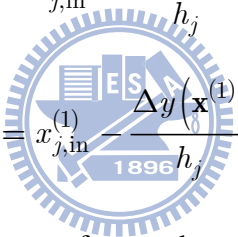
$d$  stands for the separation of every adjacent constellation, and we have

the points  $\hat{\mathbf{x}} = \mathbf{x}^{(1)}$  where  $\hat{x}_j = a$ , and  $\hat{\mathbf{x}}$  is outside the slab.

- If  $x_{j,\text{out}} \in a$ , Update  $X_{V_{\text{out}}} = \{X_{V_{\text{out}}}, \hat{\mathbf{x}}\}$  and the  $j$ th element of  $D_{V_{\text{out}}}$  corresponding to each  $\hat{\mathbf{x}}$ . If  $j$  is the last visited dimension then discard  $\mathbf{x}^{(1)}$  from the set  $X_{V_{\text{out}}}$ . Go to Step 2.
- Else, then discard  $\mathbf{x}^{(1)}$  from the set  $X_{V_{\text{out}}}$ , update  $X_{VD} = \{X_{VD}, \hat{\mathbf{x}}\}$  and the  $j$ th element of  $D_{V_{\text{out}}}$  corresponding to each  $\hat{\mathbf{x}}$ . Go back to Step 2.

Step 4: If  $X_{V_{\text{in}}}$  is empty, go to Step 1. Otherwise, we calculate

$$x_{j,\text{up}} = x_{j,\text{in}}^{(1)} - \frac{\Delta y(\mathbf{x}^{(1)})}{h_j} + C$$

$$x_{j,\text{low}} = x_{j,\text{in}}^{(1)} - \frac{\Delta y(\mathbf{x}^{(1)})}{h_j} - C,$$


where  $j$  is chosen from the unvisited dimension of  $D_{V_{\text{in}}}$

corresponding to each  $x$ .

Step 5: For each value  $x \in \{x_{j,\text{low}}, x_{j,\text{up}}\} \cap \mathbb{Z}^1$  and then we have the points

$\hat{\mathbf{x}} = \mathbf{x}^{(1)}$  where  $\hat{x}_j = x$ , and  $\hat{\mathbf{x}}$  is inside the slab.

- Update the  $j$ th element of  $D_{V_{\text{in}}}$  corresponding to each  $\hat{\mathbf{x}}$ . If  $\hat{\mathbf{x}} \notin X_{V_{\text{in}}}$  then update  $X_{V_{\text{in}}} = \{X_{V_{\text{in}}}, \hat{\mathbf{x}}\}$ , and compute the  $\text{Dist}_M$  by  $\Delta y$ .

And the value  $a \in \{\{\hat{a}_j : \max(x) + d, \tilde{a}_k : \min(x) - d\} \cap \mathbb{Z}^1\}$  and

then we have the points  $\hat{\mathbf{x}} = \mathbf{x}^{(1)}$  where  $\hat{x}_j = a$ , and  $\hat{\mathbf{x}}$  is outside

the slab.

- Update  $X_{V_{\text{out}}} = \{X_{V_{\text{out}}}, \hat{\mathbf{x}}\}$  and the  $j$ th element of  $D_{V_{\text{out}}}$  corresponding to each  $\hat{\mathbf{x}}$ . If  $j$  is the last visited dimension then discard  $\mathbf{x}^{(1)}$  from the set  $X_{V_{\text{out}}}$ . Go to Step 4.

Step 6: Each point  $\mathbf{x}$  in  $X_{\text{in}}$  falls in the slab, which is shown in **Fig. 3-1**.

The proposed search algorithm can efficiently find the valid candidate points satisfying (3.3) for a given  $C$ . Typical underdetermined decoders use all those points to find the near-ML solution by the SDA when the radius of constraints is not large. In the above description, we know the decoding complexity is closely related to the number of candidate points. However, the number of candidate points is still large with large antenna number difference. Therefore, an efficient decoder by conducting the intersectional operations with dynamic radius adaptation will be proposed in next section.

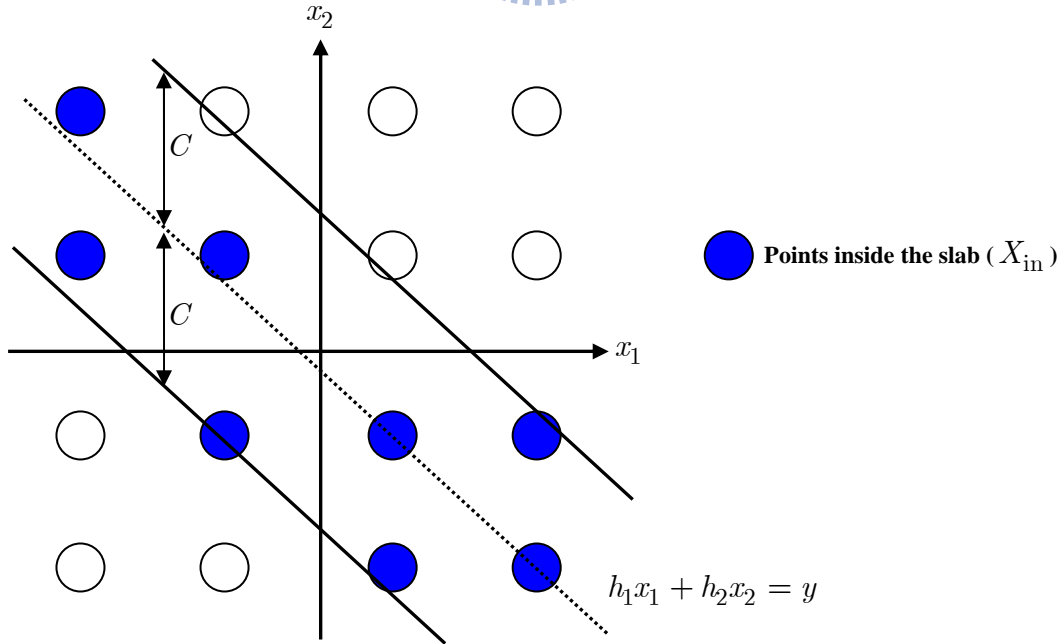


**Fig. 3-1** An example of slab with 4-PAM and  $k = 2$

## 3.2 Efficient Decoding Algorithm with Intersection of Candidate Sets

The main idea of typical underdetermined decoding algorithms is to find a candidate set in which the number of candidate points is as small as possible. The SDA is then employed to find the ML solution. The conceptual diagram is illustrated in Fig. 3-2. From Fig. 3-2, we know that the decoding complexity depends on the number of candidate points, which is positively correlated to the constellation size (e.g. 64-QAM) and antenna number difference (i.e.  $N_t - N_r$ ).

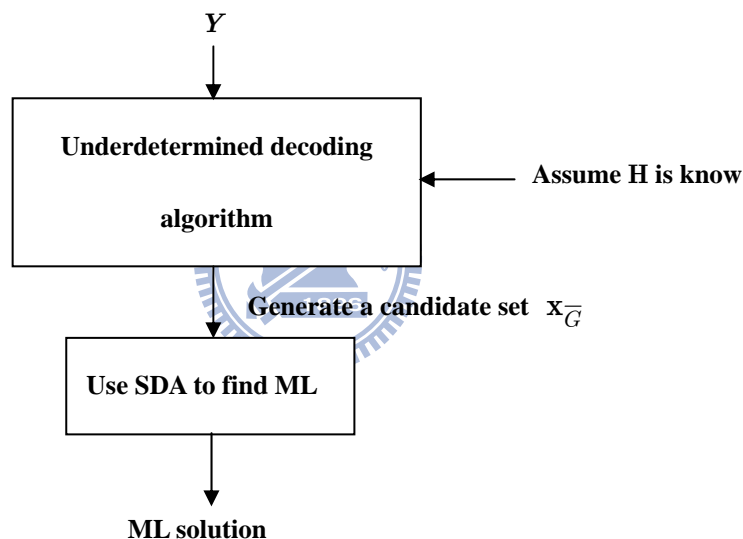


**Fig. 3-2** Block diagram of typical underdetermined decoding algorithms

We propose an efficient geometry based decoding algorithm, where (3.2) is rewritten and expanded as the summation form as follows:

$$\left\| \begin{bmatrix} y_1' \\ \vdots \\ y_{M-1}' \\ y_M' \end{bmatrix} - \begin{bmatrix} r_{1,1} & r_{1,2} & \cdots & r_{1,M-1} & r_{1,M} & \cdots & r_{1,N} \\ 0 & \ddots & \ddots & \ddots & \ddots & \ddots & \vdots \\ 0 & \cdots & 0 & r_{M-1,M-1} & r_{M-1,M} & \cdots & r_{M-1,N} \\ 0 & \cdots & 0 & 0 & r_{M,M} & \cdots & r_{M,N} \end{bmatrix} \begin{bmatrix} x_1 \\ x_2 \\ \vdots \\ x_N \end{bmatrix} \right\|^2 \leq C^2$$

$$\longrightarrow \sum_{i=1}^M \left[ y'_i - \sum_{j=i}^N r_{ij} x_j \right]^2 \leq C^2 \quad (3.5)$$

The total number of slab equations included in (3.5) is  $M$ . These equations can be written with corresponding IDs as follows:

<u>Slab equations ID</u>	<u>Slab equations</u>	
Slab $M$	$-C \leq y'_M - [r_{M,M}x_M + \dots + r_{M,N}x_N] \leq C$	
$\vdots$	$\vdots$	
Slab 2	$-C \leq y'_2 - [r_{2,2}x_2 + \dots + r_{2,N}x_N] \leq C$	(3.6)
Slab 1	$-C \leq y'_1 - [r_{1,1}x_1 + \dots + r_{1,N}x_N] \leq C,$	

In the SSD, only the last slab equation (Slab  $M$ ) is used. However, the total available number of slab equations is  $M$  in (3.6). Thus, the basic idea of the proposed method is to utilize all the available slab equations to find the candidate set, instead of only using Slab  $M$ .

Assume that  $C$  is large enough to include the ML solution and the index satisfies  $i > j$ . Using Slabs  $i$  and  $j$ , we can find two candidate sets (i.e.  $\hat{\mathbf{x}}_i, \hat{\mathbf{x}}_j$ ) which include the ML solution. Therefore, the ML solution must fall inside the intersection of the two candidate sets (i.e.  $\hat{\mathbf{x}}_{\bar{c}}$ ). This is illustrated in **Fig. 3-3**. After the slab intersection is performed, we will check the radius constraint of Slab  $i$  and  $j$  according to

$$\left\| \begin{bmatrix} y_j \\ y_i \end{bmatrix} - \begin{bmatrix} r_{j,j} & r_{j,j+1} & \dots & r_{j,i} & \dots & r_{j,N} \\ 0 & 0 & \dots & r_{i,i} & \dots & r_{i,N} \end{bmatrix} \begin{bmatrix} x_j \\ \vdots \\ x_i \\ \vdots \\ x_N \end{bmatrix} \right\|^2 \leq C^2. \quad (3.7)$$



It is inefficient to perform slab intersection and constraint checking procedure sequentially. Because the procedure requires large storage memory and many times of intersection checking for candidate points, we use another approach to achieve the same goal.

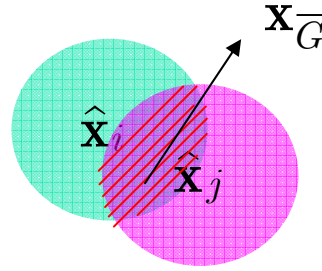


**Fig. 3-3** Illustration of intersection of candidate sets

The above procedure can be executed by the following efficient approach: we first find the candidate set  $\hat{x}_i$  and then check (3.7) with the next Slab (e.g. Slab  $j$ ). In other words, we omit the procedure of storing  $\hat{x}_j$  and matching the points of the two candidate sets, which reduces the complexity and memory storage. Therefore, we will find a new candidate set satisfying Slab  $j$  (or  $i$ ) equation in (3.6) and (3.7). There are two intersection scenarios:

**Scenario 1:** we find  $\hat{x}_i$  and check (3.7) to expand the dimensions and discard the points which does not satisfy (3.7). After that, we obtain a new candidate set.

**Scenario 2:** we first find  $\hat{x}_j$  and check (3.7). If the point of  $\hat{x}_j$  does not satisfy (3.7), we discard it. After that, we obtain a new candidate set.

In above Scenarios, we know that **Scenario 1** has lower complexity than **Scenario 2** because the average number of candidate points of  $\hat{\mathbf{x}}_i$  is smaller than that of  $\hat{\mathbf{x}}_j$ . By this reason, we expect that the number of candidate points can be as small as possible in the first candidate set just like **Scenario 1**. Therefore, we choose Slab  $M$  in (3.6) to find the first candidate set. Similarly, in order to have a lower complexity in the next procedure, we also expect that the number of points in the new candidate set can be as small as possible. By this reason, we choose Slab  $M - 1$  to be next one to intersect with Slab  $M$ , and so on. The proposed decoding algorithm guarantees to find the ML solution after performing  $M - 1$  times of the above efficient approach.

### Discussion of the radius ( $C$ )

Note that



$$C_{\min}^2 = \|\mathbf{n}\|^2 \sim \chi_N^2 \quad (3.8)$$

is Chi-square distributed with  $N$  degrees of freedom. Its cumulative distribution function is given by

$$F(x; N) = \frac{\gamma(N/2, x/2)}{\Gamma(N/2)} = P(N/2, x/2), \quad (3.9)$$

where  $\gamma(\bullet)$  is the lower incomplete Gamma function,  $\Gamma(\bullet)$  is the Gamma function, and  $P(\bullet)$  is the regularized Gamma function. In order to ensure the high efficiency of the decoder, the radius starts [10], [15] with

$$C = \sqrt{(\sigma^2) F^{-1}(\Phi + i\Delta; N)}, \quad (3.10)$$

where  $i = 0$ ,  $\Delta$  and  $\Phi$  are judiciously set, e.g.,  $\Delta = 0.001$  and  $\Phi = 0.99$ . If no points can be found within  $C$ , update  $i$  in (3.10) by  $i = i + 1$ .

The main idea of the decoding algorithm is to perform intersection of more slabs to achieve a lower decoding complexity. The procedure of the decoding algorithm is summarized as follows.

Step 1: Set  $i = M - 1$ . Use Slab  $M$  equation

$$-C \leq \mathbf{y}'_M - [R_{M,M}x_M + \cdots + R_{M,N}x_N] \leq C,$$

to find the initial candidate set  $(\hat{\mathbf{x}}_{i+1})$ . The corresponding distance  $(\text{Dist}_{i+1})$  can be obtained by the proposed search algorithm in **Section 3.1**.

Step 2: If  $i = 1$ , go to Step 4. The upper bound  $(x_{i,\text{up}})$  and lower bound  $(x_{i,\text{low}})$  of  $x_i$  corresponding to each candidate point of candidate set will be found by the radius constraint

$$\left\| \begin{bmatrix} y'_i \\ y'_{i+1} \\ \vdots \\ y'_M \end{bmatrix} - \begin{bmatrix} r_{i,i} & r_{i,i+1} & \cdots & r_{i,M} & r_{i,M+1} & \cdots & r_{i,N} \\ 0 & r_{i+1,i+1} & \cdots & r_{i+1,M} & r_{i+1,M+1} & \cdots & r_{i+1,N} \\ \vdots & \cdots & \ddots & \vdots & \ddots & \ddots & \vdots \\ 0 & \cdots & 0 & r_{M,M} & r_{M,M+1} & \cdots & r_{M,N} \end{bmatrix} \begin{bmatrix} x_i \\ x_{i+1} \\ \vdots \\ x_N \end{bmatrix} \right\| \leq C,$$

and

$$x_{i,\text{up}} = \frac{\sqrt{C^2 - (\text{Dist}_{i+1})^2} - \left( y'_i - \sum_{j=i+1}^N r_{i,j}x_j \right)}{r_{i,i}}$$

$$x_{i,\text{low}} = \frac{-\sqrt{C^2 - (\text{Dist}_{i+1})^2} - \left( y'_i - \sum_{j=i+1}^N r_{i,j}x_j \right)}{r_{i,i}}.$$

Therefore, we can easily find  $\text{Dist}_i$  through

$$\text{Dist}_i = \sqrt{\left( y'_i - \sum_{j=i}^{2N} r_{i,j}x_j \right)^2 + (\text{Dist}_{i+1})^2}.$$

Step 3: Using the upper and lower bounds corresponding to each candidate point, the new candidate set  $(\hat{\mathbf{x}}_i)$  can be constructed by

$$\hat{\mathbf{x}}_i = \left[ [x_{i,\text{low}}, x_{i,\text{up}}] \cap \mathbb{Z} \cdot [x_{i+1}, \dots, x_{2N}] \right].$$

corresponding candidate point

Choose a candidate point with minimum distance from  $\hat{\mathbf{x}}_i$  and compute the ZF-SIC solution. It gives us a new radius ( $C_{\text{new}}$ ). If  $C_{\text{new}} < C$ , update it. Set  $i = i + 1$  and go to Step 2.

Step 4: Choose a candidate point with minimum distance from  $\hat{\mathbf{x}}_1$  to be the estimate of  $\mathbf{x}$ .

Note: (1) If the initial candidate set ( $\hat{\mathbf{x}}_M$ ) is empty, increase  $C$ .  
 (2) If the candidate set ( $\hat{\mathbf{x}}_i, 1 \leq i \leq M - 1$ ) is empty, use the ZF-SIC solution as the estimate of  $\mathbf{x}$ .



### 3.3 Computer Simulation

In this section, computer simulations are conducted to evaluate the symbol-error-rate (SER) and the decoding complexity. In order to compare the complexity of the proposed decoding algorithm with other decoding algorithms, we define the complexity weights of different operations according to [15]. The weight of additions and subtractions is one if real and two if complex. Each of The multiplications and divisions is counted one if the result is real and six if it is not real. The total complexity of each simulated algorithm is the sum of the number of times of each operation multiplied by its corresponding weight. The numerical results are measured and averaged over 1000 independent channels for various average signal-to-noise ratio (SNR). In addition, the calculation of complexity also includes all preprocessing procedures (e.g. QR decomposition). We set  $\Phi = 0.99$  and

$\Delta = 0.001$  for radius  $C$  and use Schnorr and Euchner SAD (SE-SDA) [9] in SSD.

Denotes the antenna pair as  $(N_t, N_r)$ .

The average SER of using 16-QAM over various underdetermined MIMO systems using SSD and the proposed decoding algorithm are shown in **Fig. 3-4**. Note that the performance of the SSD is the same as ML detection. **Fig. 3-4** shows that the performance of the proposed decoding algorithm is close to ML performance. The proposed decoding algorithm uses the ZF-SIC solution to be the estimate of  $\mathbf{x}$  while the candidate set is empty. Therefore, the performance of the proposed decoding algorithm has slight loss at high SNR. **Fig. 3-5** shows that the complexity of the proposed decoding algorithm is lower than that of the SSD. At SNR = 15 dB, the ratios of decoding complexity of the SSD to that of the proposed decoding algorithm are 1.59, 2.03, 2.53, 3.42, corresponding to (2,1), (3,2), (4,3), (5,4). It can be observed that the ratio becomes larger with increasing number of antennas. This phenomenon is due to the fact that the increase of  $N - 1$  will lead to higher decoding complexity of the SSD. In **Fig. 3-4** and **Fig. 3-5**, we can see that the proposed decoder reduces the decoding complexity without degrading the decoding performance.

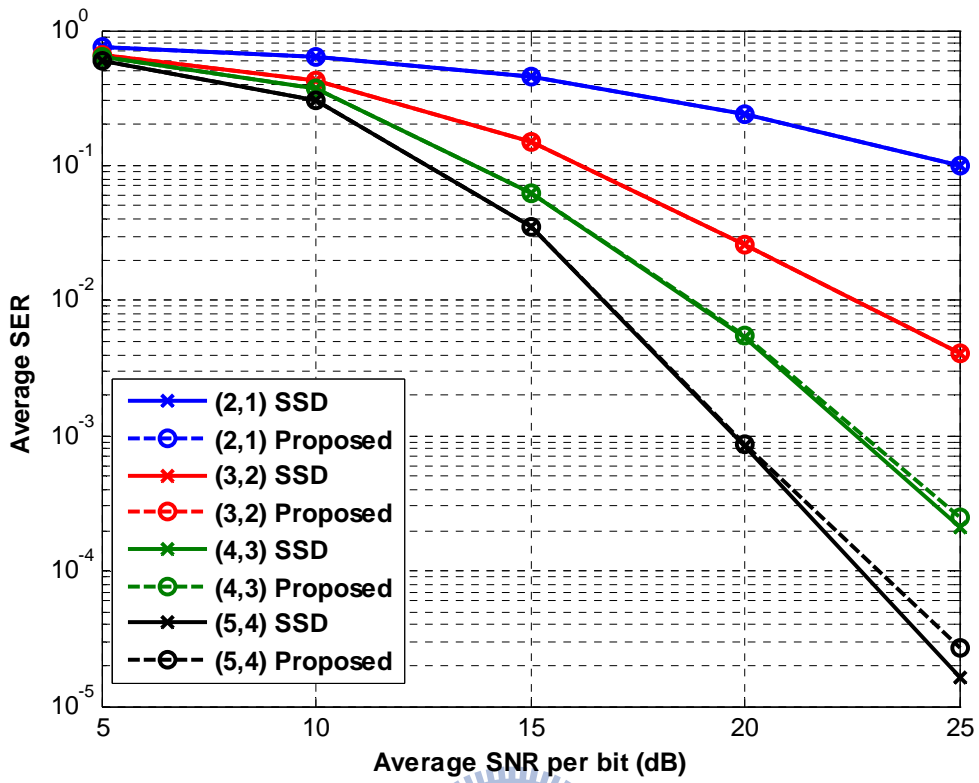


Fig. 3-4 SER comparison of SSD and the proposed method using 16-QAM

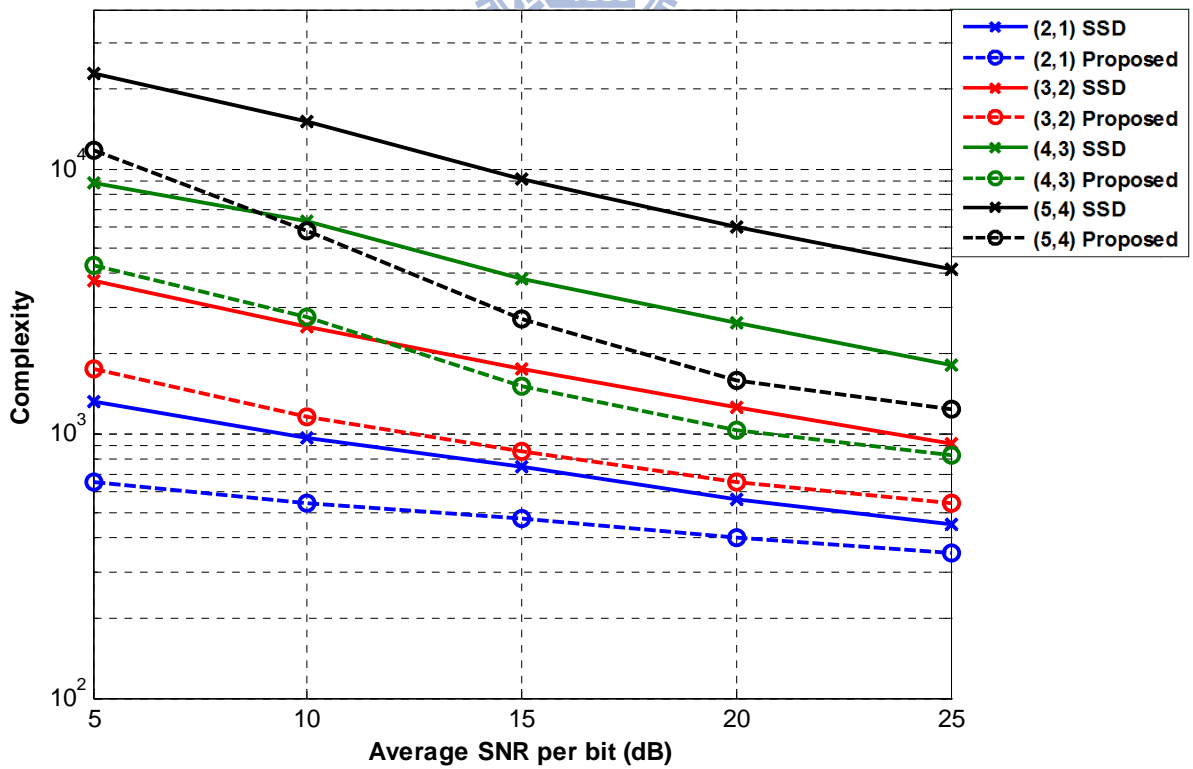
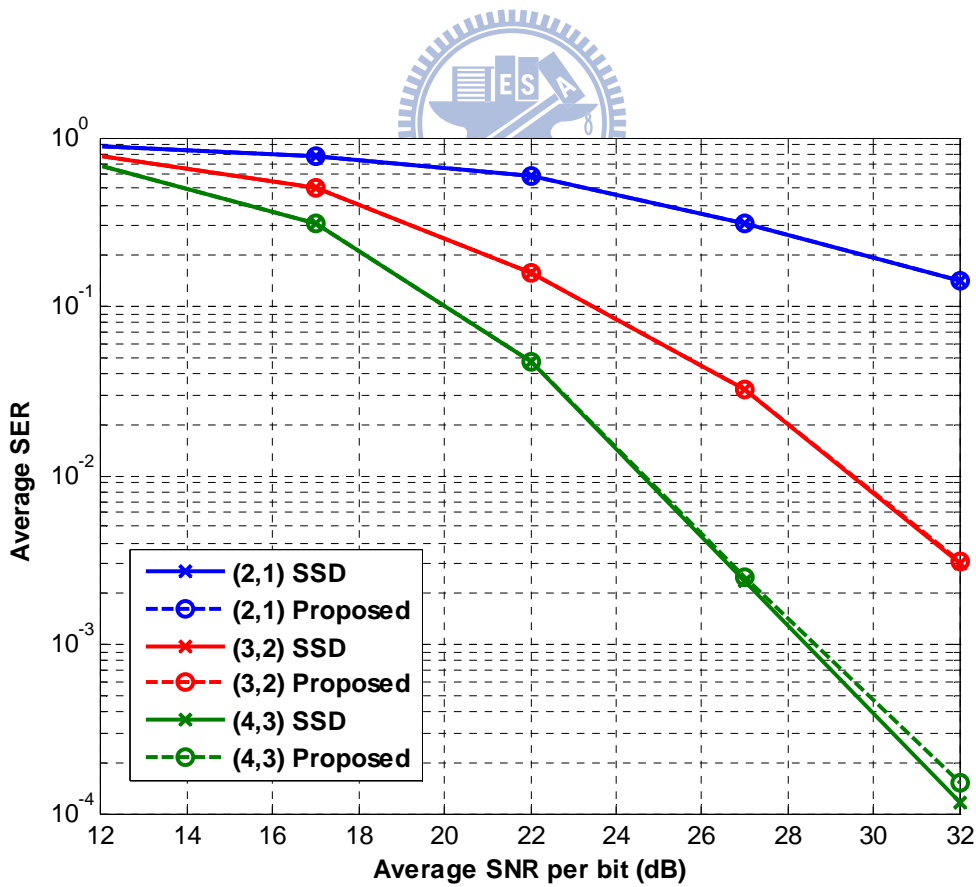


Fig. 3-5 Complexity comparison of SSD and the proposed method using 16-QAM

Here, we use 64-QAM modulation instead of 16-QAM. The average SER is shown **Fig. 3-6**. The decoding performance is close to the ML solution and still has slight loss at high SNR. **Fig. 3-7** shows that the complexity of the proposed decoding algorithm is still lower than SSD. At SNR = 27 dB, the ratios of decoding complexity of the SSD to that of the proposed decoding algorithm are 1.92, 2.21 and 4.14 corresponding to (2,1), (3,2) and (4,3). The increasing ratio phenomenon is the same as using 16-QAM. However, the reduction of complexity is larger than using 16-QAM. It means that the proposed decoder is suitable for the systems using large constellation. In **Fig. 3-6** and **Fig. 3-7**, we can see that the proposed decoder reduces the decoding complexity especially for a large number of antennas and large constellation size. Moreover, the proposed decoder also provides a near-ML solution.



**Fig. 3-6** SER comparison of SSD and the proposed method using 64-QAM

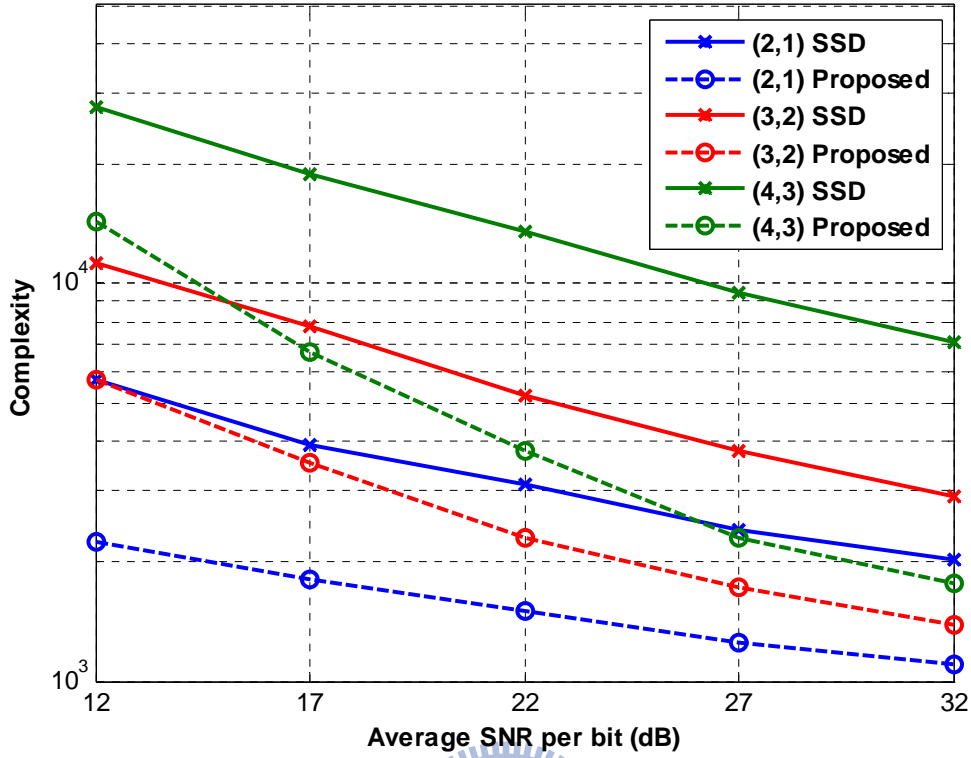


Fig. 3-7 Complexity comparison of SSD and the proposed method using 64-QAM

### 3.4 Summary

In this chapter, we give the detailed description of the proposed efficient search method which combines the PDA and SLA of SSD. The proposed search algorithm works more efficiently than the search algorithm of SSD (PDA+SLA), especially under a large constellation (i.e. 64-QAM) and a large number of antenna difference ( $N_t - N_r$ ), which is shown in **Section 3.1**. In **Section 3.2**, we propose a novel underdetermined decoding technique. The proposed decoder incorporating the proposed search method works more efficiently than SSD and obtains a near-ML performance.



# Chapter 4

## Preprocessing of Proposed Decoding Algorithm

In Chapter 3, we know that the decoding complexity of the proposed decoding algorithm depends on the number of candidate points ( $N_p$ ) of the initial candidate set.

In order to reduce the decoding complexity, we want  $N_p$  to be as small as possible for the proposed decoding algorithm. To ensure this, we propose a preprocessing scheme to further reduce the decoding complexity. Furthermore, we will give a detail analysis of the decoding complexity.

In this Chapter, we first introduce the proposed preprocessing scheme. The details of the proposed preprocessing will be introduced in Sections 4.1. In Section 4.2, we discuss the decoding complexity with different antenna pairs. The decoding complexity and performance simulations will be presented in Section 4.3 to show that the proposed preprocessing can further reduce the decoding complexity.

## 4.1 Preprocessing

In underdetermined MIMO systems, the channel matrix is preprocessed with some techniques, which can reduce the decoding complexity or improve the performance of the SDA. There are many preprocessing techniques such as lattice reduction [20-22], column permutation [22], and scaling [23]. However, we cannot apply these preprocessing techniques to reduce the decoding complexity in the proposed decoder in Chapter 3 over the underdetermined MIMO systems. In Section 3.2, we know that the primary decoding complexity results from the intersection of candidate sets (3.7). Therefore, we want the procedure of intersection is executed as few times as possible.

First, we define the number of candidate points ( $N_p$ ) inside the initial slab as an index of decoding complexity. Therefore, the  $N_p$  is expected to be as small as possible. We rewrite the initial slab form as

$$-C \leq \mathbf{y}'_M - [r_{M,M}x_M + \dots + r_{M,N}x_N] \leq C. \quad (4.1)$$

The initial slab candidates can be found by channel columns reordering, and the number of the candidates is  $C(N, N - M + 1)$ . Choosing the initial slab from the candidates is important for the proposed decoder. Geometrically speaking,  $|\mathbf{y}'_M|$  represents the distance from the origin to the slab, as shown in **Fig. 4-1**. In **Fig. 4-1**, we assume that the slab equation form is  $h_1x_1 + h_2x_2 = y$ , where  $h_i$  is a constant and  $y$  is a variable, and we define  $|\mathbf{y}'_M|$  as the location index of slab ( $\xi$ ). **Fig. 4-1** shows that  $N_p$  is small when  $\xi$  is large. Therefore, we want to choose the slab from the candidates with the maximum  $\xi$  to be the initial slab.

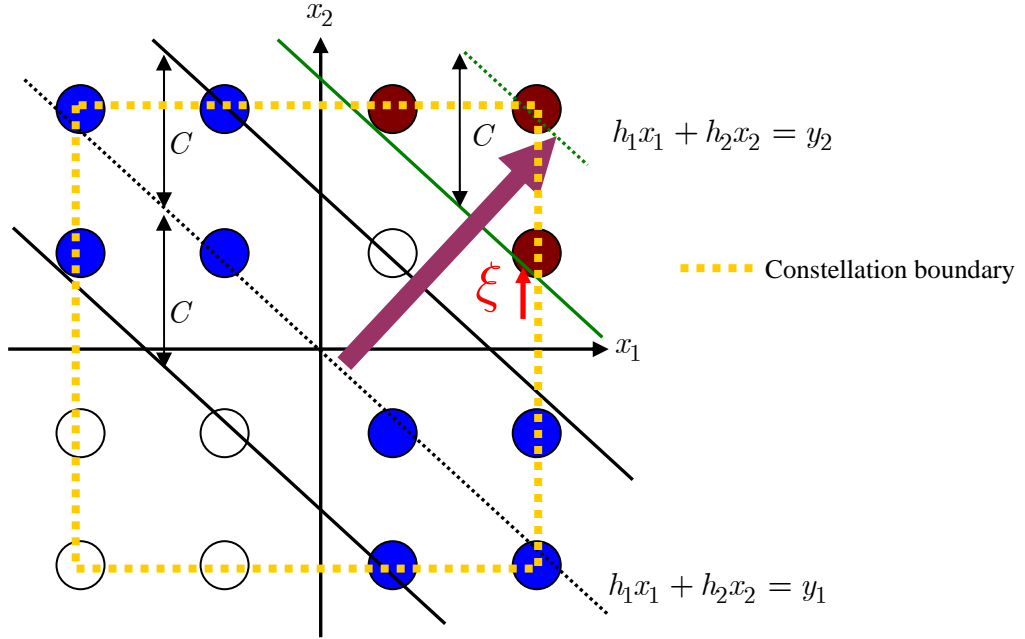


**Fig. 4-1** Geometrical diagram of slabs with different  $y$



There is one issue needed to be addressed: how to find  $\xi$  of each initial slab efficiently? We propose an efficient approach for this issue, which is summarized as follows:

We rewrite  $\mathbf{y}' = \mathbf{Q}^T \mathbf{y} \in \mathbb{R}^M$  of (3.2)

$$\mathbf{y}' = [y'_1 \quad y'_2 \quad \cdots \quad y'_M]^T = [\bar{\mathbf{q}}_1^T \mathbf{y} \quad \bar{\mathbf{q}}_2^T \mathbf{y} \quad \cdots \quad \bar{\mathbf{q}}_M^T \mathbf{y}]^T \in \mathbb{R}^M, \quad (4.2)$$

where  $\mathbf{Q} = [\bar{\mathbf{q}}_1 \quad \bar{\mathbf{q}}_2 \quad \cdots \quad \bar{\mathbf{q}}_M] \in \mathbb{R}^{M \times M}$ . Here, we focus on finding  $y'_M$ , which can be obtained by computing  $\bar{\mathbf{q}}_M$ . Since different reorderings of channel columns result in different  $\bar{\mathbf{q}}_M$ , the problem becomes how to find  $\bar{\mathbf{q}}_M$  efficiently. The channel column reordering is formed as  $\mathbf{HP}$ , where  $\mathbf{P}$  is a permutation matrix.

Step 1:  $\mathbf{P} = \mathbf{I}$ , therefore  $\mathbf{HP} = \mathbf{H} = [\tilde{\mathbf{h}}_1 \tilde{\mathbf{h}}_2 \cdots \tilde{\mathbf{h}}_N]$ . The detail of the QR

decomposition of  $\mathbf{HP}$  is given as follows:

$$\mathbf{V}_1 \mathbf{H} = \begin{bmatrix} \mathbf{T}_1 & \mathbf{A} \\ \mathbf{0} & \tilde{\mathbf{H}}_1 \end{bmatrix}, \quad (4.3)$$

where  $\mathbf{V}_1$  is  $M \times M$  Householder matrix of the first column vector of  $\mathbf{H}$ ,  $\mathbf{T}_1$  is a scalar and  $\tilde{\mathbf{H}}_1 = \mathbf{V}_1[2:M, 1:M] \mathbf{H}[1:M, 2:M]$ . Then define  $\tilde{\mathbf{H}}_1 \in \mathbb{R}^{M-1 \times M-1}$  to be a new matrix to perform the same procedure as follows:

$$\mathbf{V}_2 \tilde{\mathbf{H}}_1 = \begin{bmatrix} \mathbf{T}_2 & \mathbf{A} \\ \mathbf{0} & \tilde{\mathbf{H}}_2 \end{bmatrix}, \quad (4.4)$$

where  $\mathbf{V}_2$  is  $(M-1) \times (M-1)$  Householder matrix of the first column vector of  $\tilde{\mathbf{H}}_1$ ,  $\mathbf{T}_2$  is a scalar and  $\tilde{\mathbf{H}}_2 = \mathbf{V}_2[2:M-1, 1:M-1] \tilde{\mathbf{H}}_1[1:M-1, 2:M-1]$ . And so on, we can obtain QR composition of  $\mathbf{H}$  as

$$\mathbf{Q}^T \mathbf{H} = \mathbf{R}, \quad (4.5)$$

where

$$\mathbf{Q}^T = \begin{bmatrix} \tilde{\mathbf{q}}_1^T \\ \tilde{\mathbf{q}}_2^T \\ \vdots \\ \tilde{\mathbf{q}}_M^T \end{bmatrix} = \mathbf{U}_{M-1} \cdots \mathbf{U}_2 \mathbf{U}_1$$

and

$$\mathbf{U}_i = \begin{bmatrix} \mathbf{I} & \mathbf{0} \\ \mathbf{0} & \mathbf{V}_i \end{bmatrix}.$$

Since we only consider  $\bar{\mathbf{q}}_M$ , we compute the last row of  $\mathbf{U}_{M-1}$  to yield to following:

$$\begin{bmatrix} \otimes \\ \vdots \\ \otimes \\ \bar{\mathbf{q}}_M^T \end{bmatrix} = \begin{bmatrix} \mathbf{I} & \mathbf{0} & \mathbf{0} \\ \mathbf{0} & \otimes & \otimes \\ \mathbf{0} & v_{M-1(2,1)} & v_{M-1(2,2)} \end{bmatrix} \Omega_1, \quad (4.6)$$

where  $\Omega_1 = \mathbf{U}_{M-2} \cdots \mathbf{U}_1$ . To avoid unnecessary computations, we only consider the last two rows of  $\Omega_1$ . Therefore, we compute the last two rows of  $\mathbf{U}_{M-2}$  as

$$\Omega_1 = \begin{bmatrix} \mathbf{I} & 0 & 0 & 0 \\ 0 & \otimes & \otimes & \otimes \\ 0 & v_{M-2(2,1)} & v_{M-2(2,2)} & v_{M-2(2,3)} \\ 0 & v_{M-2(3,1)} & v_{M-2(3,2)} & v_{M-2(3,3)} \end{bmatrix} \Omega_2, \quad (4.7)$$

where  $\Omega_2 = \mathbf{U}_{M-3} \cdots \mathbf{U}_1$ . By iterating this procedure, we can obtain  $\bar{\mathbf{q}}_M$  with  $\mathbf{P} = \mathbf{I}$ .

From (4.2)  $y_M'$  can be found accordingly.

Step 2: We can find  $y_M'$  of another order of channel columns quickly after Step 1 is performed. For example, assuming that the order of channel columns is to exchange  $\bar{\mathbf{h}}_{M-1}$  and  $\bar{\mathbf{h}}_M$  as  $[\bar{\mathbf{h}}_1 \cdots \bar{\mathbf{h}}_M \bar{\mathbf{h}}_{M-1} \bar{\mathbf{h}}_{M+1} \cdots \bar{\mathbf{h}}_N]$ . We can observe that only  $\mathbf{U}_{M-1}$  is required to be computed. This concept can be used to find  $y_M'$  of other orderings of the channel columns. Therefore, we choose the slab from the candidates with the maximum  $\xi$  to be the initial slab.

## 4.2 Alternative Approach of Preprocessing

The preprocessing scheme in Section 4.1 is to perform an exhaustive search for all  $\xi$ . Therefore, the computational complexity is large when the number of candidates ( $C(N, N - M + 1)$ ) is large. In this section, we propose another approach of preprocessing to avoid the exhaustive search. We know that the size of channel matrix  $\mathbf{H}$  is  $M \times N$  where  $M < N$ , so the rank of  $\mathbf{H}$  is  $M$ . Span the columns of  $\mathbf{H}$  as

$$\begin{aligned} S &= \text{span}(\text{cols of } \mathbf{H}) = \text{span}(\bar{\mathbf{h}}_1 \bar{\mathbf{h}}_2 \cdots \bar{\mathbf{h}}_N) \\ &= \text{span}(\bar{\mathbf{v}}_1 \bar{\mathbf{v}}_2 \cdots \bar{\mathbf{v}}_M) \in \mathbb{R}^M, \end{aligned} \quad (4.8)$$

where  $S$  is a space spanned from the columns of  $\mathbf{H}$ . The set of  $\bar{\mathbf{v}}_i$  is a basis set of  $\mathbf{H}$ .

In this approach, the goal is to find the slab with a large  $\xi$ , but not the maximum one. In other words, we want the basis  $\bar{\mathbf{q}}_M$  to have a high correlation to  $y$  from (4.2) and rewrite it as follows

$$\mathbf{y}' = [y'_1 \ y'_2 \ \cdots \ y'_M]^T = [\bar{\mathbf{q}}_1^T \mathbf{y} \ \bar{\mathbf{q}}_2^T \mathbf{y} \ \cdots \ \bar{\mathbf{q}}_M^T \mathbf{y}]^T = \mathbf{R}\mathbf{x} + \mathbf{n}' \in \mathbb{R}^M, \quad (4.9)$$

where  $\mathbf{Q} = [\bar{\mathbf{q}}_1 \ \bar{\mathbf{q}}_2 \ \cdots \ \bar{\mathbf{q}}_M] \in \mathbb{R}^{M \times M}$  is a unitary matrix. Those column vectors in  $\mathbf{Q}$  can be a basis set of  $\mathbf{H}$ . In Section 4.1, the QR decomposition of  $\mathbf{H}$  is performed by Householder process (Householder-QRD). In this section, we consider that the QR decomposition of  $\mathbf{H}$  is performed by Gram-Schmidt process (GS-QRD). The detail of GS-QRD is summarized as follows.

## GS-QRD

Consider the Gram-Schmidt procedure. The columns vectors of the matrix  $\mathbf{A}$  is considered in the process as follows

$$\mathbf{A} = [\bar{\mathbf{a}}_1, \bar{\mathbf{a}}_2, \dots, \bar{\mathbf{a}}_n].$$

Then,

$$\bar{\mathbf{u}}_1 = \bar{\mathbf{a}}_1, \quad \bar{\mathbf{v}}_1 = \bar{\mathbf{u}}_1 / \|\bar{\mathbf{u}}_1\|,$$

$$\bar{\mathbf{u}}_2 = \bar{\mathbf{a}}_2 - (\bar{\mathbf{a}}_2 \bar{\mathbf{v}}_1) \bar{\mathbf{v}}_1, \quad \bar{\mathbf{v}}_2 = \bar{\mathbf{u}}_2 / \|\bar{\mathbf{u}}_2\|,$$

⋮

$$\bar{\mathbf{u}}_{k+1} = \bar{\mathbf{a}}_{k+1} - (\bar{\mathbf{a}}_{k+1} \bar{\mathbf{v}}_1) \bar{\mathbf{v}}_1 - \dots - (\bar{\mathbf{a}}_{k+1} \bar{\mathbf{v}}_k) \bar{\mathbf{v}}_k, \quad \bar{\mathbf{v}}_{k+1} = \bar{\mathbf{u}}_{k+1} / \|\bar{\mathbf{u}}_{k+1}\|,$$

where  $\|\bullet\|$  is the 2-norm. The resulting QR decomposition is

$$\mathbf{A} = \begin{bmatrix} \bar{\mathbf{v}}_1 & \bar{\mathbf{v}}_2 & \dots & \bar{\mathbf{v}}_n \end{bmatrix} \begin{bmatrix} \bar{\mathbf{a}}_1 \cdot \bar{\mathbf{v}}_1 & \bar{\mathbf{a}}_2 \cdot \bar{\mathbf{v}}_1 & \dots & \bar{\mathbf{a}}_n \cdot \bar{\mathbf{v}}_1 \\ 0 & \bar{\mathbf{a}}_2 \cdot \bar{\mathbf{v}}_2 & \dots & \bar{\mathbf{a}}_n \cdot \bar{\mathbf{v}}_2 \\ \vdots & \vdots & \ddots & \vdots \\ 0 & 0 & \dots & \bar{\mathbf{a}}_n \cdot \bar{\mathbf{v}}_n \end{bmatrix} = \mathbf{QR}.$$

In the above GS-QRD, we can determine the ordering of  $\bar{\mathbf{q}}_i$  of  $\mathbf{Q}$ , by the procedure as follows. First, Choose the lowest correlation between  $y$  and  $\bar{\mathbf{h}}_i$  from the column vectors of  $\mathbf{H}$ . Set the chosen  $\bar{\mathbf{h}}_i$  to be the first basis  $\bar{\mathbf{q}}_1$ . Therefore, the value of  $|y_1|$  is smaller than other selections. Second, the remaining  $\bar{\mathbf{h}}_j$  will be updated by  $\bar{\mathbf{h}}_i$  as follows

$$\bar{\mathbf{h}}_j^{(1)} = \bar{\mathbf{h}}_j - \bar{\mathbf{h}}_j \cdot \bar{\mathbf{q}}_1 \quad j \neq i. \quad (4.10)$$

Finally, we repeat the above procedure, the ordering of  $\mathbf{H}$  will be determined. The detail procedure of the preprocessing is summarized as follows.

Step 1: Initialize the vector set  $V = \{\bar{\mathbf{h}}_i, i = 1, 2, \dots, N\}$  and  $k = 1$ .

Step 2: Choose the lowest correlation between  $y$  and  $\bar{\mathbf{h}}_i$  from  $V$  and set it to be  $\bar{\mathbf{q}}_k$ .

Step 3: Discard  $\bar{\mathbf{h}}_i$  from  $V$  and update  $V$

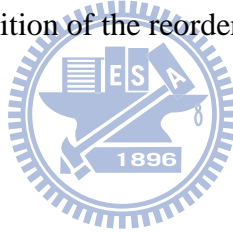
$$\bar{\mathbf{h}}_j^{(1)} = \bar{\mathbf{h}}_j - \bar{\mathbf{h}}_j \cdot \bar{\mathbf{q}}_j \quad j \neq i,$$

and  $k = k + 1$ . Go to Step 2.

Step 4: Compute

$$r_{jk} = \bar{\mathbf{q}}_j \bar{\mathbf{h}}_k, \quad j = 1, 2, \dots, k - 1.$$

The QR decomposition of the reordering  $\mathbf{H}$  is obtained.



In **Fig. 4-2** simulation, the 16-QAM is used,  $N_t = 3$  and  $N_r = 2$  under SNR = 15 dB. Denote the preprocessing by Householder in Section 3.1 as Method I and the preprocessing by GS-QRD as Method II. We investigate the probability density function of  $|y_m|$  and make comparisons between the cases without preprocessing, Method I and Method II, as shown in **Fig. 4-2**. **Fig. 4-2** shows that the value of  $|y_m|$  without preprocessing is the lowest. This means that the slab locates on the central of the constellation area, it implies that the mean of  $N_p$  without preprocessing is large than the  $N_p$  of Method I and Method II. **Fig. 4-2** also shows that the probability density function of  $|y_m|$  with Method II is almost same as Method I.



In the following simulation, the 4-QAM is used,  $N_t = 3, 4, 5, 6$  and  $N_r = 2$  under SNR = 15 dB. The reduced percentage of Method I and Method II compared with no preprocessing are shown in **Fig. 4-3**. Since Method II does not perform exhaustive search for  $|y_m|$ , the proposed method has smaller reduced percentage. **Fig. 4-3** shows the reduced percentage is larger with the increasing antenna number difference. This phenomenon is due to the fact that the value of  $|y_m|$  becomes larger when the antenna number difference increasing. Therefore, the reduced percentage saturates when the number of transmit antennas is too large.

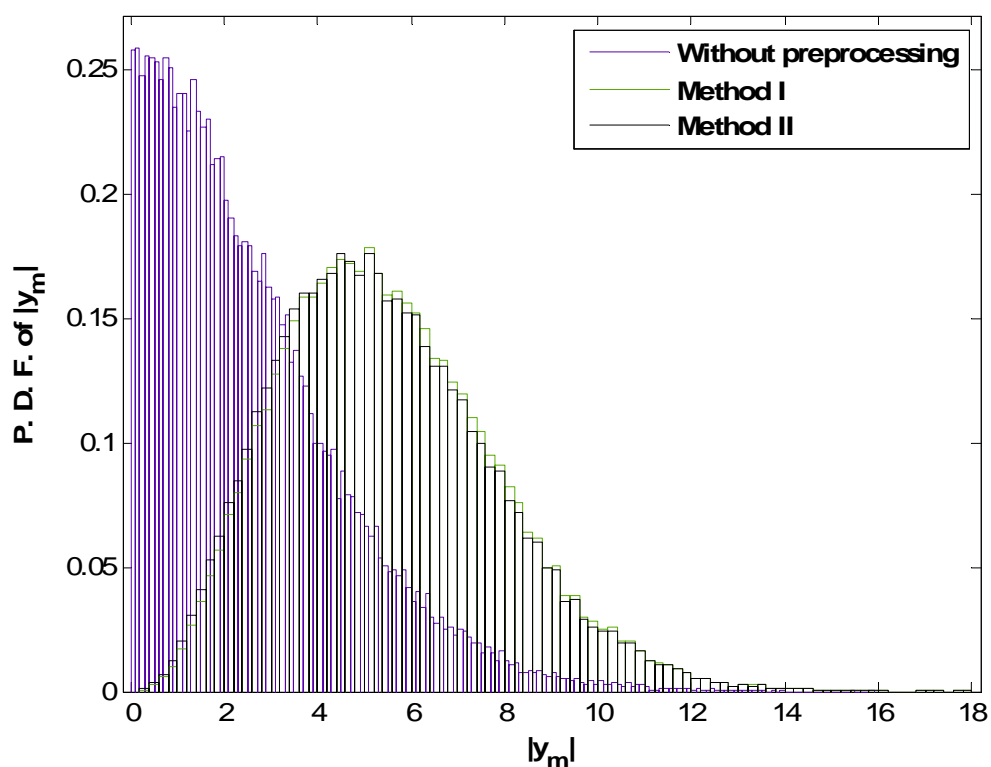


**Fig. 4-2** Probability density function of  $|y_m|$

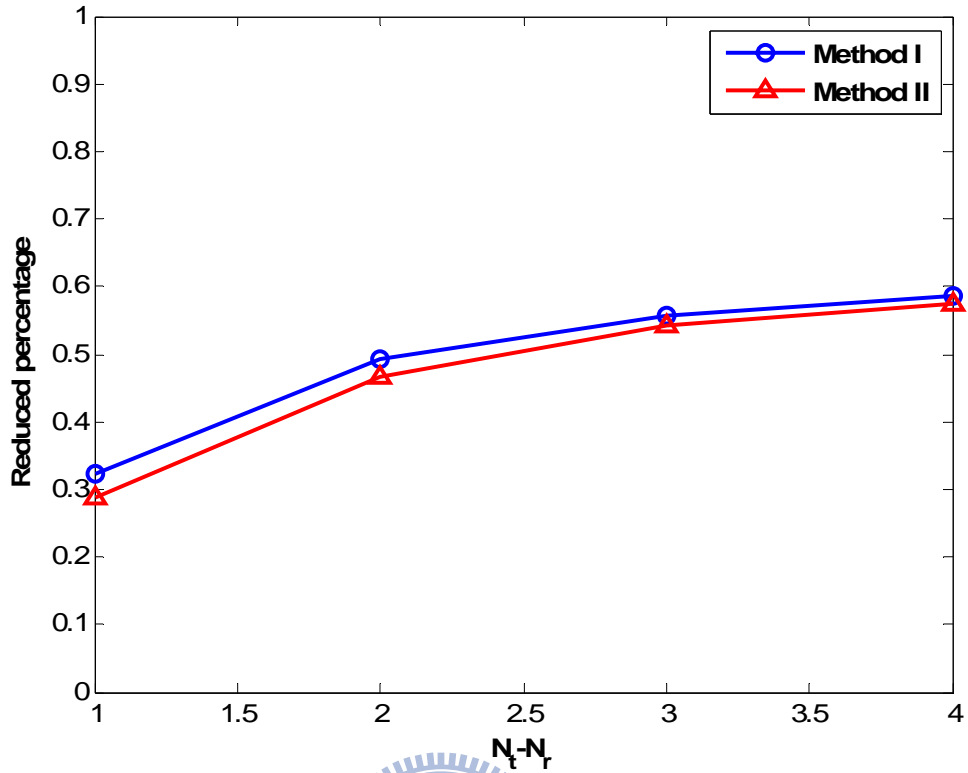


Fig. 4-3 The reduced percentage of Method I and Method II

## 4.3 Computer Simulations

In this section, computer simulations are conducted to evaluate the performance of SER and decoding complexity. The complexity weights of different operations are the same as in Section 3.3. The total complexity of each simulated algorithm is the sum of the number of times of each operation multiplied by its corresponding weight. The numerical results are measured and averaged over 1000 independent channels for various average SNRs. In addition, the calculation of complexity also includes all preprocessing procedures. We set  $\Phi = 0.99$  and  $\Delta = 0.001$  for radius  $C$  and use SE-SDA in SSD. The Method II preprocessing is used in the proposed decoder.

The average SER of using 64-QAM over various underdetermined MIMO systems using the proposed decoding algorithm with Method II preprocessing and without preprocessing are shown **Fig. 4-4**. The performance of the proposed decoding algorithm is also close to the performance of ML. The major difference between the proposed decoding algorithm with and without preprocessing is the channel ordering. Therefore, the different ZF-SIC solutions are found, the SER are slightly different at high SNR. **Fig. 4-5** shows that the complexity of the proposed decoding algorithm with preprocessing is lower than the proposed decoding algorithm without preprocessing. This phenomenon is due to the fact that the number of initial candidate set points with preprocessing is smaller than that without preprocessing; this result is given in Section 4.3. Since the preprocessing improves less at high SNR, the reduced percentage of decoding complexity at low SNR is larger than at high SNR. However, the preprocessing complexity is still large with large the number of antennas. This leads to the complexity of the proposed decoder with preprocessing is dominated by the additional preprocessing complexity. In **Fig. 4-4** and **Fig. 4-5**, we can see that the decoding complexity of the proposed decoder with preprocessing is further reduced especially at low SNR without degrading decoding performance.

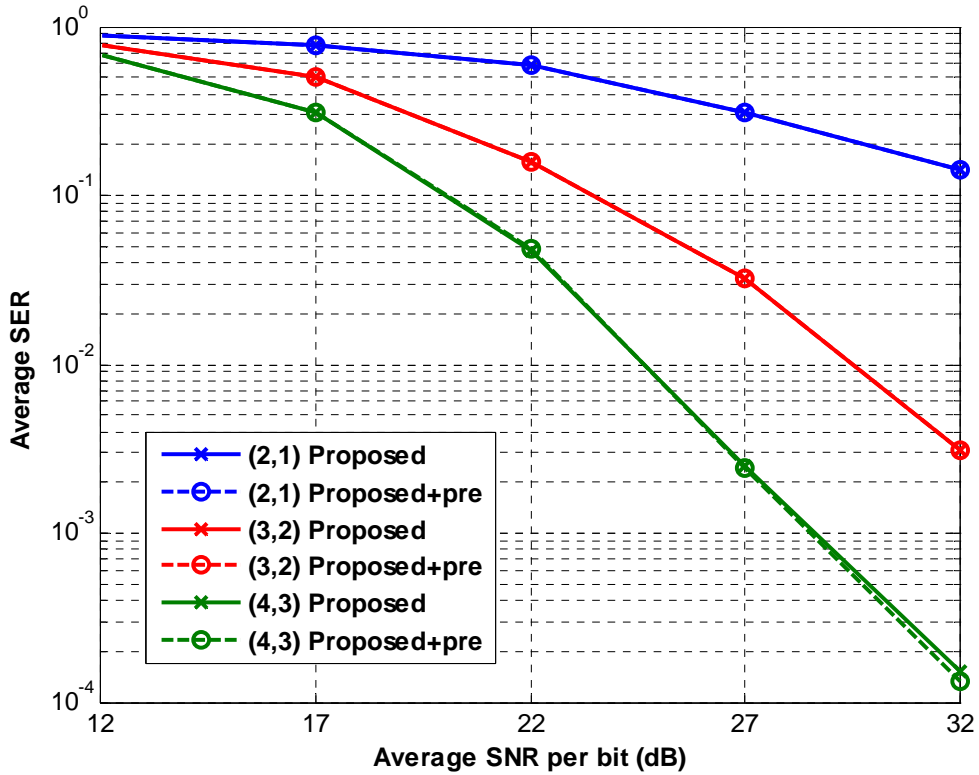


Fig. 4-4 SER comparison of proposed method with and without preprocessing

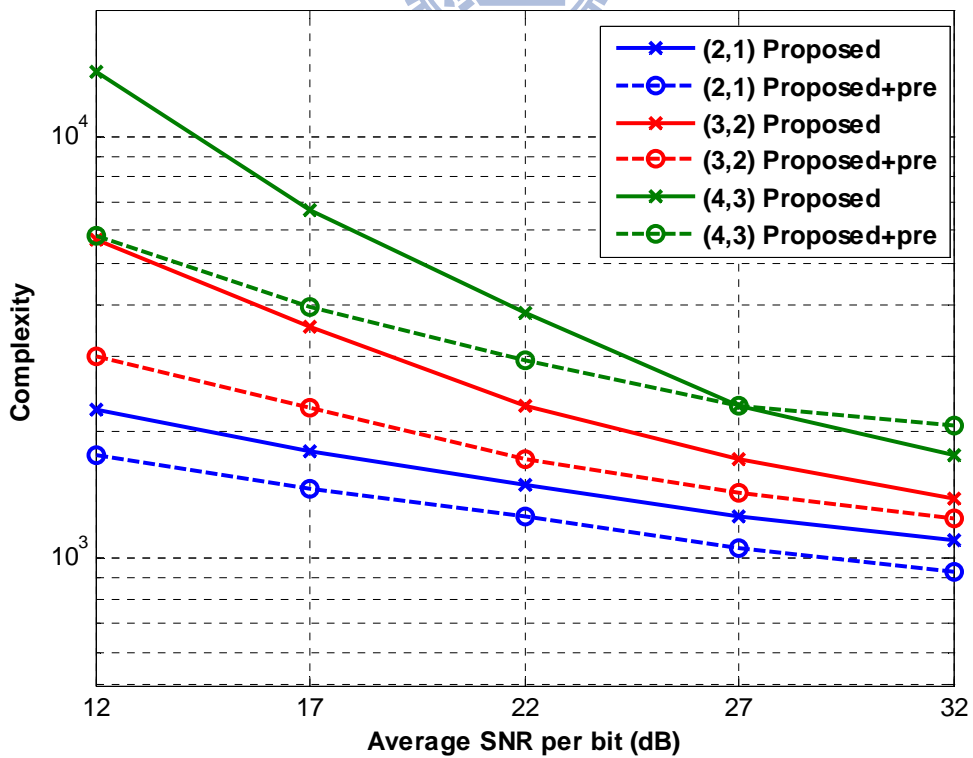
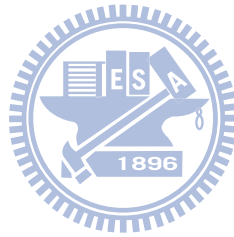


Fig. 4-5 Complexity comparison of proposed method with and without preprocessing

## 4.4 Summary

In this chapter, we provide two preprocessing schemes to further reduce the decoding complexity. In Section 4.1, we propose an exhaustive search of  $|y_m|$  which can find the maximum  $|y_m|$ . This leads to the preprocessing complexity is too high. To reduce the preprocessing complexity, we propose an alternative approach in Section 4.2. The method finds a large  $|y_m|$ , but not the necessarily maximum  $|y_m|$ . In Section 4.3, we simulate the SER and the complexity of the proposed decoder with preprocessing and compare it with the proposed decoder without preprocessing. Simulations show that the proposed decoder with preprocessing has a lower complexity than the proposed decoder without preprocessing without degrading the decoding performance.



# Chapter 5

## Conclusions and Future Works

In the beginning, this thesis reviews some important MIMO techniques and typical decoding algorithms for MIMO systems. The GSD achieves the ML performance; however, its decoding complexity is exponentially increasing with the antenna number difference ( $N_t - N_r$ ). Recently, the SSD is considered as an efficient decoding algorithm. However, there are two drawbacks of the SSD: search method of the SSD is not efficient and the number of valid candidate points is usually large. These lead to high decoding complexity. Hence, the goal of this thesis is aiming at the reduction of decoding complexity of the SSD without degrading its decoding performance.

In Chapter 3, we propose another approach of search algorithms to find the valid candidate points in Section 3.1. In Section 3.2, an efficient decoding algorithm is proposed by conducting the intersectional operations with dynamic radius adaptation. With a large constellation size, the decoding complexity of the proposed decoding algorithm is significantly lower than that of the SSD. Simulations demonstrate that the proposed decoding algorithm has a lower decoding complexity than the SSD, and achieves a near-ML performance.

Since the decoding complexity is sensitive to the number of candidate points ( $N_p$ ) of the initial candidate set, we want  $N_p$  to be as small as possible. In Chapter 4, two preprocessing schemes for the proposed decoding algorithm are provided to further reduce the decoding complexity by reducing  $N_p$ . First, the proposed Householder QR decomposition based preprocessing scheme which performs an exhaustive search for the location index of slab ( $\xi$ ) is introduced in Section 4.1. To reduce the computational complexity of the preprocessing, an alternative approach is provided in Section 4.2. Simulations show that the proposed decoding algorithm with the GS based preprocessing further reduces the decoding complexity. The main contributions of this thesis are as follows. First, the proposed decoding algorithm reduces the decoding complexity of SSD. Second, the proposed preprocessing scheme can further reduce the decoding complexity of the proposed decoder especially for a large constellation size. In the case of 64-QAM and  $4 \times 3$  MIMO, the decoding complexity of proposed decoder can save up to 76% compared to SSD. If the proposed preprocessing is used, the decoding complexity of proposed decoder can save up to 79% compared to SSD.

There are some future works worthy of further investigation. The first one is that the MIMO channel information is assumed to be perfectly known. However, the MIMO channel cannot be precisely estimated in practice. The second one is to find the mathematic analysis of the decoding complexity. Finally, finding a new approach to further reduce the preprocessing complexity is an important issue.

# Bibliography

- [1] E. Telatar, "Capacity of multi-antenna Gaussian channels," *AT&T Bell Labs Internal Tech. Memo.*, June 1995.
- [2] G. J. Foschini, "Layered space-time architecture for wireless communication in a fading environment when using multi-element antennas," *AT&T Bell Labs Tech. J.*, pp. 41-59, Autumn 1996.
- [3] S. M. Alamouti, "A simple transmit diversity technique for wireless communications," *IEEE J. Select. Areas Commun.*, vol. 16, no. 8, pp. 1451-1458, Oct. 1998.
- [4] G. J. Foschini and M. J. Gans, "On limits of wireless communications in a fading environment when using multiple antennas," *Wireless Personal Commun.*, vol. 6, no.3, pp. 311-335, Mar. 1998.
- [5] A. J. Goldsmith and S. G. Chua, "Variable-rate variable-power MQAM for fading channels," *IEEE Trans. Commun.*, vol. 45, no.10, pp. 1218-1230, Oct. 1997.
- [6] S. Catreux, V. Erceg, D. Gesbert and R. W. Heath, "Adaptive modulation and MIMO coding for broadband wireless data networks," *IEEE Commun. Mag.*, vol. 40, no. 6, pp. 108-115, June 2002.
- [7] G. J. Foschini, G. D. Golden, R. A. Valenzuela and P. W. Wolniansky, "Simplified processing for high spectral efficiency wireless communication employing multi-element arrays," *IEEE J. Select. Areas Commun.*, vol. 17, no. 11, pp. 1841-1852, Nov. 1999.
- [8] G. D. Golden, G. J. Foschini, R. A. Valenzuela and P. W. Wolniansky, "Detection algorithm and initial laboratory results using V-BLAST space-time communication architecture," *Electronic Letters*, vol. 35, no. 1, pp. 14-16, Jan. 1999.



- [9] C. P. Schnorr and M. Euchner, "Lattice basis reduction: improved practical algorithms and solving subset sum problems," *Math. Programming*, vol. 66, pp. 181-191, Aug. 1994.
- [10] B. Hassibi and H. Vikalo, "On the sphere-decoding algorithm I. expected complexity," *IEEE Trans. Signal Process.*, vol. 53, no. 8, pp. 2806-2818, Aug. 2005.
- [11] M. O. Damen, K. Abed-Meraim, and J.-C. Belfiore, "A generalised sphere decoder for asymmetrical space-time communication architecture," *IEE Electronics Letters*, vol. 36, no. 2, pp. 166-167, Jan. 2000.
- [12] K. K. Wong and A. Paulraj, "Near maximum-likelihood detection with reduced-complexity for multiple-input single-output antenna systems," in *Proc. Asilomar Conf. on Signals, Systems, and Computers*, Nov. 2004.
- [13] Z. Yang, C. Liu, and J. He, "A new approach for fast generalized sphere decoding in MIMO systems," *IEEE Signal Processing Letters*, vol. 12, no. 1, pp. 41-44, Jan. 2005.
- [14] K. K. Wong and A. Paulraj, "Efficient near maximum-likelihood detection for underdetermined MIMO antenna systems using a geometrical approach," *EURASIP Journal on Wireless Commun. and Networking*, Oct. 2007.
- [15] K. K. Wong, A. Paulraj and R. D. Murch, "Efficient high-performance decoding for overloaded MIMO antenna systems," *IEEE Trans. Wireless Commun.*, vol. 6, no. 5, pp. 1833-1843, May 2007.
- [16] T. M. Cover and J. A. Thomas, *Elements of Information Theory*, John Wiley & Son, Inc., 1991.
- [17] P. W. Wolniansky, G. J. Foschini, G. D. Golden and R. A. Valenzuela, "V-BLAST: An architecture for realizing very high data rates over the rich-scattering wireless channel," in *Proc. URSI ISSSE-98*, pp. 295-300, Sep. 1998.

- [18] U. Fincke and M. Phost, "Improved methods for calculating vectors of short length in a lattice, including a complexity analysis," *Math. of Comp.*, vol. 44, pp. 463–471, Apr. 1985.
- [19] E. Viterbo and J. Boutros, "A universal lattice code decoder for fading channels," *IEEE Trans. Inf. Theory*, vol. 45, pp. 1639–1642, July 1999.
- [20] A. K. Lenstra, H. W. Lenstra and L. Lovasz, "Factoring polynomials with rational coefficients," *Math. Ann.*, vol. 261, no. 4, pp. 513-534, July 1982.
- [21] C. Windpassinger and R. Fischer, "Low-complexity near maximum likelihood detection and precoding for MIMO systems using lattice reduction," in *Proc. IEEE Information Theory Workshop*, Paris, France, pp. 345–348, Apr. 2003.
- [22] W. Zhao and G. B. Giannakis, "Reduced complexity closest point decoding algorithms for random lattices," *IEEE Trans. Wireless Commun.*, vol. 5, no. 1, pp. 101-111, Jan. 2006.
- [23] K. Lee and J. Chun, "ML symbol detection based on the shortest path algorithm for MIMO systems," *IEEE Trans. Signal Process.*, vol. 55, no. 11, pp. 5477-5484, Nov. 2007.

